Plant immune system activation is necessary for efficient root colonization by auxin-secreting beneficial bacteria

Elhanan Tzipilevich,[1,2] Dor Russ,[3,4] Jeffery L. Dangl,[3,4] and Philip N. Benfey[1,2,5,*]

[1]Department of Biology, Duke University, Durham, NC 27708, USA
[2]Howard Hughes Medical Institute Duke University, Durham, NC 27708, USA
[3]Department of Biology, University of North Carolina at Chapel Hill, Chapel Hill, NC 27599, USA
[4]Howard Hughes Medical Institute. University of North Carolina at Chapel Hill, Chapel Hill, NC 27599, USA
[5]Lead contact
*Correspondence: philip.benfey@duke.edu
https://doi.org/10.1016/j.chom.2021.09.005

SUMMARY

Although plant roots encounter a plethora of microorganisms in the surrounding soil, at the rhizosphere, plants exert selective forces on their bacterial colonizers. Unlike immune recognition of pathogenic bacteria, the mechanisms by which beneficial bacteria are selected and how they interact with the plant immune system are not well understood. To better understand this process, we studied the interaction of auxin-producing *Bacillus velezensis FZB42* with *Arabidopsis* roots and found that activation of the plant immune system is necessary for efficient bacterial colonization and auxin secretion. A feedback loop is established in which bacterial colonization triggers an immune reaction and production of reactive oxygen species, which, in turn, stimulate auxin production by the bacteria. Auxin promotes bacterial survival and efficient root colonization, allowing the bacteria to inhibit fungal infection and promote plant health. Thus, a feedback loop between bacteria and the plant immune system promotes the fitness of both partners.

INTRODUCTION

Plant roots interact with a plethora of bacteria in the surrounding soil. Extensive efforts have characterized the diversity of these bacterial species (Bai et al., 2015; Lundberg et al., 2012). Bacteria can have pathogenic, beneficial, or neutral effects on plants. Bacterial diversity is reduced when moving from bulk soil to the root surface (rhizosphere) and further into the root interior (endosphere), indicating that plants exert selective forces on their colonizing bacteria. An early filter used by plants to recognize and respond to bacteria and other organisms is its immune system (Couto and Zipfel, 2016), which utilizes receptors to recognize bacterial molecules called MAMPs (microbe-associated molecular patterns). These include flagella, peptidoglycans, bacterial elongation factor TU, and others (Jones and Dangl, 2006; Zipfel, 2014). Recognizing these molecules leads to a cascade of molecular events. The earliest stages of this response include an efflux of calcium ions and a burst of reactive oxygen species (ROS) (Zipfel, 2009). This is followed by phosphorylation events that lead to the induction of immune-related genes (Spoel and Dong, 2012). Plant immune system recognition and activation have been extensively characterized in the context of pathogenic bacteria (Dodds and Rathjen, 2010; Xin et al., 2018). However, MAMP receptors recognize molecules found in all bacteria, and beneficial bacteria can induce an immune response similar to the pathogenic ones (e.g., Colaianni et al., 2021; Stringlis et al., 2018). The influence of the immune system on the healthy root microbiome and how beneficial bacteria respond to the plant immune system is an active area of research, and much remains to be learned (Chen et al., 2020; Hacquard et al., 2017; Teixeira et al., 2019). To better understand this process, we studied the interaction of *Bacillus velezensis FZB42* (*B. velezensis*) with the root of the model plant *Arabidopsis thaliana* (*Arabidopsis*). *B. velezensis* is a model Gram-positive soil bacterium, which synthesizes a plethora of secondary metabolites shown to inhibit the growth of plant pathogens (Chowdhury et al., 2015). It also synthesizes auxin (Fan et al., 2018), a plant hormone that influences many aspects of plant growth (Zhao, 2010). A well-characterized response of exogenous auxin addition is the arrest of primary root growth and stimulation of lateral root formation (Banda et al., 2019). *B. velezensis* was shown to stimulate lateral root formation and biomass accumulation in several plant species, including *Arabidopsis*, *Lemna minor*, and lettuce, in an auxin-dependent manner (Chowdhury et al., 2013; Fan et al., 2011; Idris et al., 2007). The effects of auxin secreted by bacteria on plant growth have been explored for decades. Bacterial auxin can manipulate plant growth (Mashiguchi et al., 2019; Spaepen et al., 2014), probably providing the bacteria with access to nutrients. Bacterial auxin can also inhibit the plant immune system through antagonistic interaction

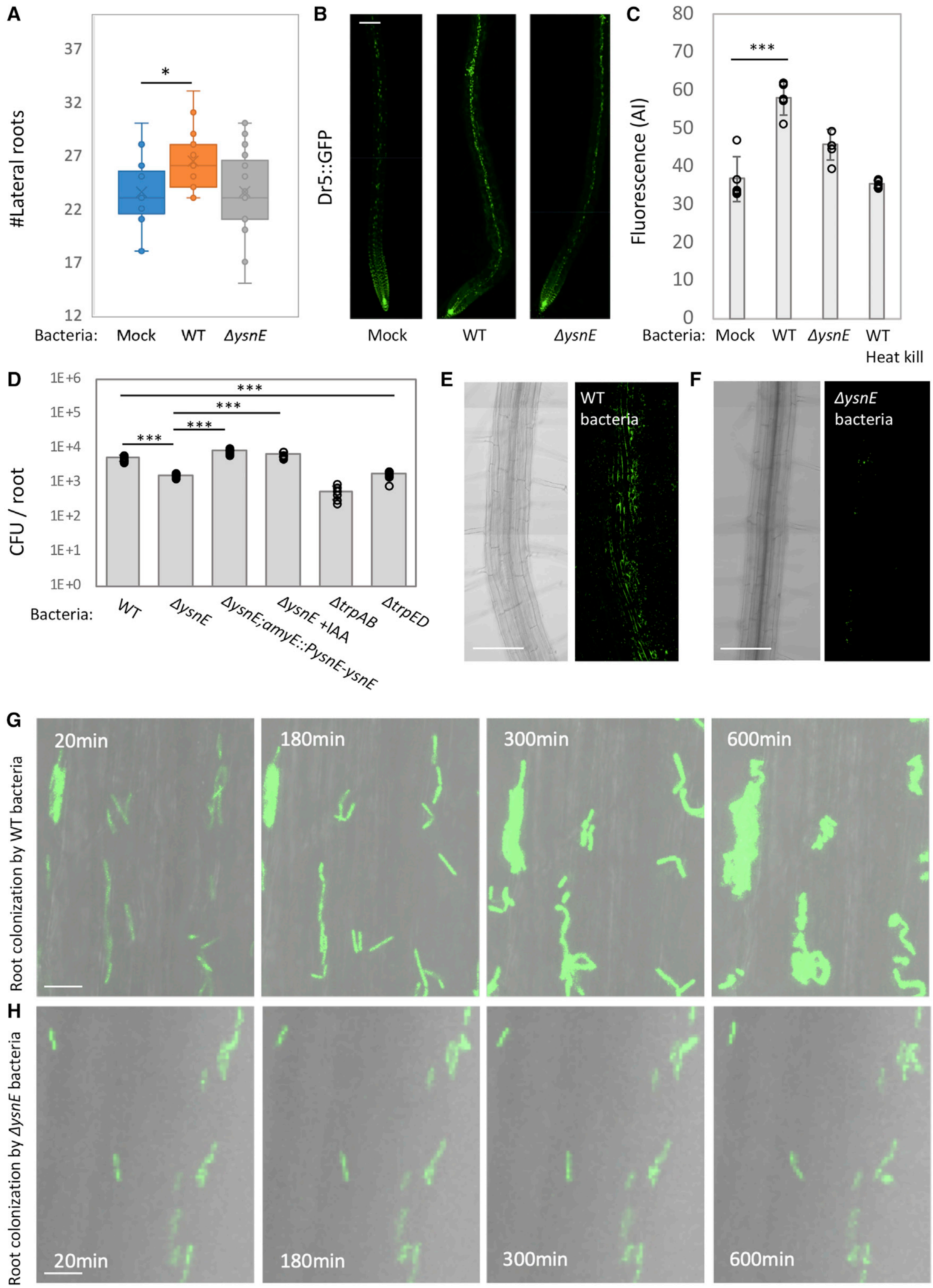

Figure 1. Bacterial auxin stimulates plant lateral root formation and bacterial root colonization

(A) Seedlings were inoculated with either WT, *ΔysnE* bacteria, or buffer (mock) on agar plates for 7 days and the number of lateral roots was counted. ($n \geq 20$) (*$p < 0.05$, ANOVA followed by post hoc Tukey Kramer).

(B and C) Arabidopsis DR5::GFP reporter lines were inoculated with the indicated bacterial strains for 48 h on agar plates.

(B) 100× maximal projection confocal images of GFP fluorescence from DR5::GFP expression.

(legend continued on next page)

with the salicylic-acid signaling pathway (Kunkel and Harper, 2018). However, it is unclear if the production of auxin by bacteria has a direct effect on their colonization capacity (Duca et al., 2014; Patten and Glick, 1996). We found that a positive feedback between the plant immune system and bacterial auxin secretion occurs during root colonization. Immune system modulation by bacteria triggers ROS production by the plant, which, in turn, activates auxin secretion by the bacteria. This secreted auxin is necessary for bacterial survival in media containing elevated ROS levels, and for colony formation on the root. An efficient colony formation enables the bacteria to fight pathogenic fungi and enhance plant health. Thus, our work reveals that bacterial auxin directly impacts its capacity for root colonization and uncovers a positive influence of the plant immune system on bacterial colonization with beneficial effects for the plant.

RESULTS

Bacterial auxin plays a dual role during root colonization

To characterize the interaction between bacteria and plant roots, we inoculated *B. velezensis* onto Arabidopsis seedlings growing on agar plates. Consistent with previous results (Fan et al., 2011; Idris et al., 2007), after 7 days of incubation, colonized plants exhibited reduced primary root growth and increased lateral root emergence (Figures 1A, S1A, and S1B) in comparison with seedlings treated with the buffer (mock), a response consistent with bacterial auxin secretion (e.g., Spaepen et al., 2014). Plants expressing an auxin response reporter (DR5::GFP Liao et al., 2015) revealed increased auxin response in roots inoculated with *B. velezensis* (Figures 1B and 1C). The root phenotype was dependent on bacterial auxin secretion, as plants inoculated with a strain of *B. velezensis* deficient in auxin production (*ΔysnE* (Idris et al., 2007), see Figure S1C) did not exhibit primary root growth inhibition or lateral root stimulation (Figures 1A, S1A, and S1B) and had reduced DR5::GFP fluorescence (Figures 1B and 1C).

ΔysnE bacteria failed to colonize the root as efficiently as WT bacteria, indicating that bacterial auxin not only triggers a root developmental response but is also necessary for efficient root colonization (Figures 1D–1F). Complementation of YsnE in *trans* (*ΔysnE; amyE::*P_{ysnE}*YsnE*) restored auxin production (Figure S1C) and root colonization (Figure 1D). Similarly, the addition of exogenous auxin (IAA) also restored *ΔysnE* bacterial colonization (Figure 1D). Similar results were obtained with two other mutants in the auxin biosynthesis pathway, *ΔtrpAB* and *ΔtrpED* (Idris et al., 2007) (Figure 1D). *ΔysnE* bacteria exhibited normal growth *in vitro* (Figure S1D), normal swarming motility (Figure S1E), and biofilm formation (Figure S1F), indicating that these processes, which can influence root colonization (Chen et al., 2013; Dietel et al., 2013), and are not responsible for the reduced colonization capacity. In an attempt to elucidate the underlying cause, we performed time-lapse microscopy of root colonization by WT and *ΔysnE* GFP-expressing bacteria (Fan et al., 2011). Although most of the WT bacteria replicated and formed colonies over the root (Figure 1G), *ΔysnE* bacteria failed to replicate (Figure 1H). We conclude that bacterial auxin is necessary for *B. velezensis* to survive and replicate on the root.

Auxin is necessary for *B. velezensis* to antagonize the plant immune reaction

The reduced ability of *ΔysnE* bacteria to colonize the root (Figure 1H) led us to hypothesize that *B. velezensis* is able to trigger a plant immune response (see also Xie et al., 2017). Auxin produced by pathogenic bacteria has previously been shown to reduce the plant immune response (McClerklin et al., 2018). RNA sequencing of whole roots after 48 h of bacterial colonization (Table S1) revealed that gene categories related to immune system activation, such as camalexin synthesis and callose deposition, were enriched in the root transcriptome as compared with buffer-inoculated roots (mock) (Figure 2A; Table S2). These early response results were corroborated by increased expression of immune-related promoters (pPER5, pFRK1) fused to fluorescent reporters (Zhou et al., 2020) (Figures 2B and 2C), as well as callose deposition (Figures S2A and S2B), indicating that *B. velezensis* colonization elicits an immune reaction. Monitoring plant ROS production also revealed a significant response (Figure 2D).

To identify the pathway by which the immune response is triggered, we measured the ROS response in plants deficient in three different MAMP receptors—*fls2*, mutant in the receptor for bacterial flagella (Zipfel et al., 2004), *efr2*, mutant in the receptor for bacterial elongation factor TU (Zipfel et al., 2006), and *lym1,lym3*, mutant in the receptor for bacterial peptidoglycan (Willmann et al., 2011). We found that *efr2* and *fls2* exhibited a significant reduction in ROS production (Figure 2B). These results are consistent with the similarity between elf18 and flg22 and their respective epitopes in the *B. velezensis* genome (70.6% and 66.7% identity, respectively, Figure S2C). *efr2* also exhibited a reduction in callose deposition (Figures S2A and S2B). We hypothesized that if bacterial auxin is necessary to antagonize the plant immune response, then the colonization of bacteria deficient in auxin production would be restored on mutant plants with compromised immunity. Consistent with

(C) Quantification of GFP fluorescence from maximum intensity projection images. Shown are averages and SD n = 5, each circle represents one root. (***p < 0.005, two-tailed t test with Bonferroni correction) Scale bar, 50 μm

(D) Seedlings were inoculated with the indicated bacterial strains with or without 5 μM IAA (for *ΔysnE* bacteria) for 48 h on agar plates and the number of colonizing bacteria was counted. Shown are averages and SD (log_{10} transformed); each circle represents an average of 3 technical replicates from the same root, (***p < 0.005, two-tailed t test with Bonferroni correction).

(E and F) Seedlings were inoculated with either WT or *ΔysnE* bacteria expressing GFP (*amyE::Pspac-gfp*) for 48 h on agar plates. Shown are 200× maximal projection confocal images of DIC (differetial interference contrast) from roots (left panels) and GFP fluorescence from bacteria (right panels) for WT (E) and *ΔysnE* (F) bacteria. Scale bars, 50 μm.

(G and H) Seedlings were inoculated with either WT (G) or *ΔysnE* (H) bacteria expressing GFP (*amyE::Pspac-gfp*) and followed by time-lapse confocal microscopy for 12 h. Shown are 400× maximal projection overlaid images of DIC from roots (gray) and GFP fluorescence from bacteria (green), taken at the indicated time points. Yellow arrows highlight bacterial growth arrest, probably culminating in cell death. Red arrows highlight *ΔysnE* bacteria replicating away from the root plane. Scale bars, 10 μm.

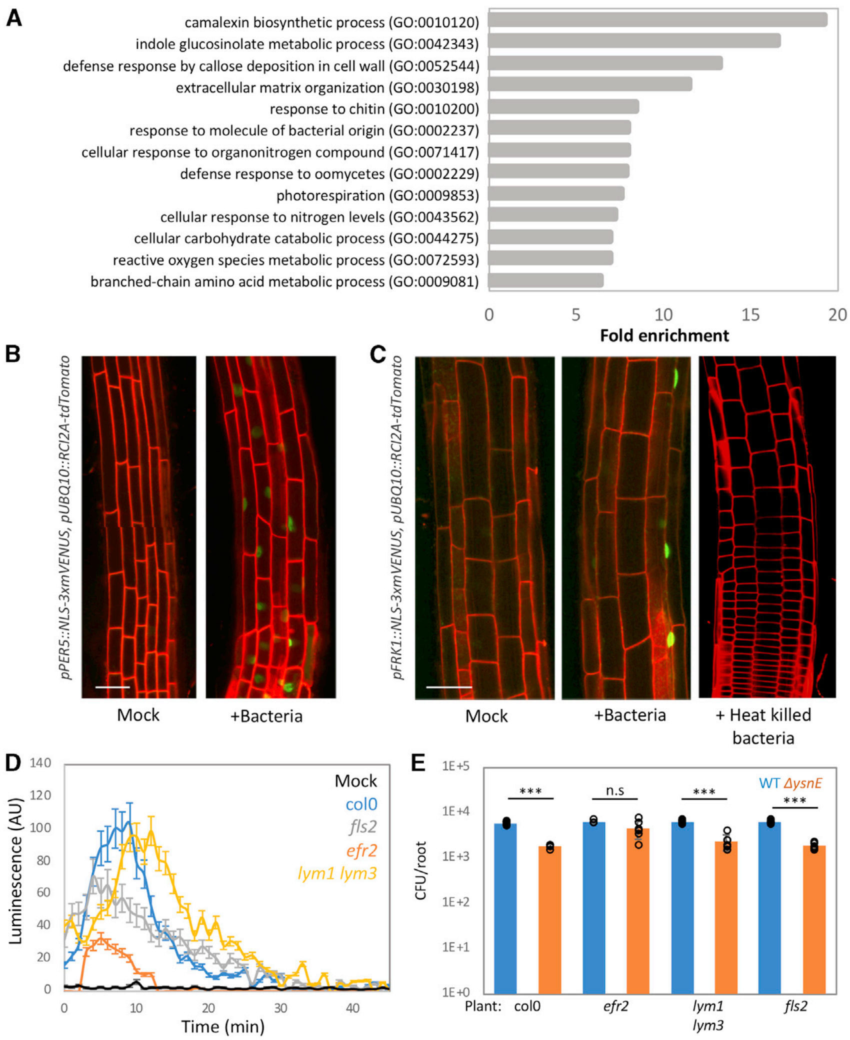

Figure 2. *B. velezensis* triggers an immune response in an EFR dependent manner

(A) Representative biological process GO term analysis of plant genes upregulated in response to *B. velezensis* colonization. p < 0.05 (see Table S2 for the full list of GO categories).

(B and C) Seedlings of the indicated genotypes, were inoculated with bacteria or buffer alone (mock) for 48 h. Shown are 400× overlay images of *pUBQ10::RCI2A-tdTomato* (red) and *pPER5::NLS-3xmVENUS* (green) (B), or *pFRK1::NLS-3xmVENUS* (green) (C). Representative roots from five roots from each condition. Scale bars, 25 μm.

(D) Leaf discs from 28-day-old plant taken from the indicated plant genotypes were incubated with bacteria adjusted to OD 0.1, and the ROS burst was measured. Shown are averages and SD ($n \geq 10$). *efr* and, to a lesser extent, *fls2* exhibited significant reductions in ROS response, ($p < 0.05$, ANOVA followed by post hoc Tukey Kramer).

(E) Seedlings from the indicated genotypes were inoculated with either WT or *ΔysnE* bacteria for 48 h on agar plates and the number of colonizing bacteria was counted. Shown are averages and SD of 2 independent experiments (log_{10} transformed) with n = 3 for each, each circle represents an average of 3 technical replicates from the same root, (***$p < 0.005$, two-tailed t test with Bonferroni correction).

this hypothesis, we found that *ΔysnE* growth was significantly enhanced on *efr2* mutant plants (Figures 2E, 3A, 3B, and S2D) but, interestingly, not on *fls2* plants. Although these auxin-deficient bacteria are able to replicate on *efr2* mutant plants, unlike WT bacteria, they do not adhere to the root (compare Figures 3A, 3B, and 1G). The EFR receptor is expressed in the roots at very low levels (Figure 3C) (Wu et al., 2016; Zhou et al., 2020). However, *B. velezensis* colonization highly stimulated the expression of a pEFR transcriptional reporter (Figure 3C). Intriguingly, exogenous IAA also stimulated pEFR reporter expression (Figure 3C), suggesting that bacterial auxin is also able to stimulate EFR expression. We conclude that EFR restricts the growth of *ΔysnE* bacteria, and auxin is able to overcome this restriction.

Auxin antagonizes ROS toxicity

To identify the components of plant immunity perturbed by bacterial auxin, we monitored *ΔysnE* bacterial colonization on mutants in immune response genes. Mutations in SALK_068675, an additional *efr* mutant allele, restored *ΔysnE* bacterial colonization. Moreover, a *bak1-5* mutant, defective in multiple MAMP receptor activation, as well as *crt3*, mutant in a gene essential for EFR receptor function (Li et al., 2009), restored *ΔysnE* bacterial colonization (Figure S3A). Neither perturbation in the indoleglucosinolate and camalexin synthesis pathway (*myb51* Frerigmann et al., 2014 and *cyp71a13*, Mucha et al., 2019) nor the defects in plant stress hormone effectors (*npr1-5*, *ein2-5*, *jar1-1*) affected *ΔysnE* bacterial colonization (Figure S3A). The lack of SA response (*npr1-5* Ding and Ding, 2020) is notable, as auxin is known to antagonistically interact with the SA pathway to enhance the colonization of *P. syringae* (McClerklin et al., 2018; Robert-Seilaniantz et al., 2011). In contrast, the growth of auxin-deficient bacteria was restored on *rbohd rbohf* plants, which are defective in immune triggered ROS production (Figure 3D) (Torres et al., 2005). Moreover, significant recovery of *ΔysnE* bacterial colonization was obtained when ROS production was chemically inhibited by DPI (Tsukagoshi et al., 2010) (Figure S3B). These results suggest that bacterial auxin antagonizes plant ROS production to enable root colonization.

On *rbohd rbohf* plants, *B. velezensis* caused a negative effect with a significant increase in root colonization (Figure 3D), reduced the number of lateral roots and smaller plants (Figures S3C and S3D). We hypothesize that *efr2* plants, although perturbed in *B. velezensis* triggered immunity are still capable of eliciting a sufficiently strong immune response with ROS production (Figure 2B) to keep the bacteria from overgrowing the plant.

ROS are toxic molecules utilized by the plant to kill invading pathogens and to signal cells neighboring infection sites to induce defense pathways (e.g., Fones and Preston, 2012). NADPH oxidase enzymes, such as RbohD and RbohF, produce

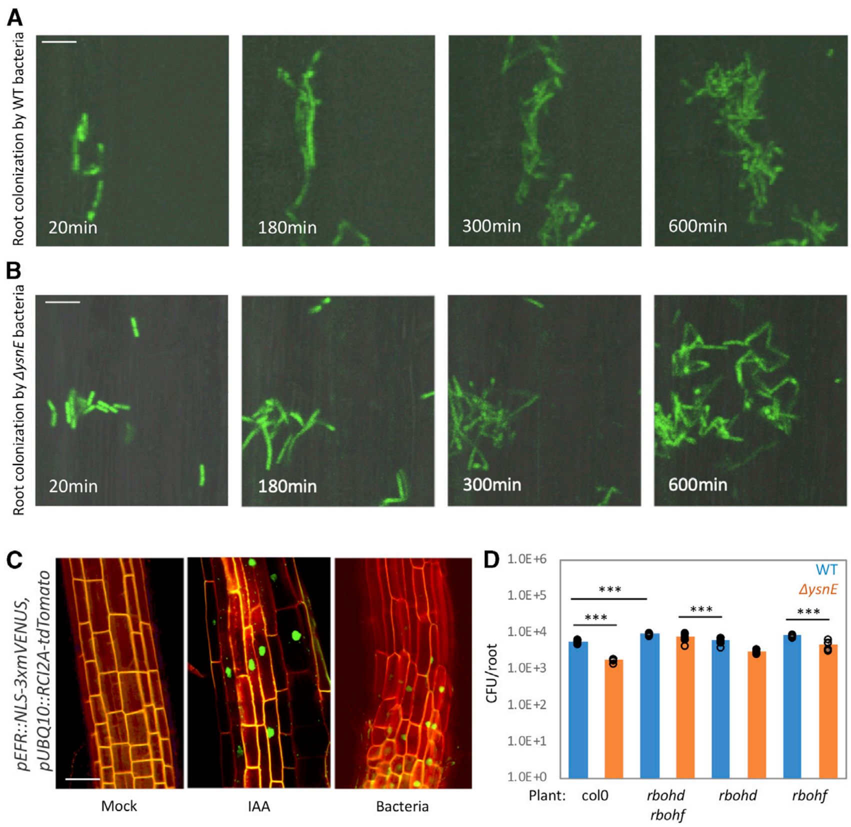

Figure 3. Bacterial auxin counteracts the plant immune response

(A and B) Seedlings were inoculated with either WT (A) or *ΔysnE* bacteria (B) expressing GFP (*amyE::P-spac-gfp*) and followed by time-lapse confocal microscopy for 12 h. Shown are 400× overlay images of DIC from roots (gray) and GFP fluorescence from bacteria (green), taken at the indicated time points. *ΔysnE* bacteria replicated over the root but failed to adhere in a manner similar to WT bacteria (also compare to Figure 1G). Scale bar, 10 μm.

(C) Seedlings of *pEFR::NLS-3xmVENUS, pUBQ10::RCl2A-tdTomato* were inoculated with WT bacteria, grown in the presence of 5 μM IAA or buffer for 48 h. Shown are 400× representative overlay images of *pUBQ10::RCl2A-tdTomato* (cell wall, red) and *pEFR::NLS-3xmVENUS* (EFR-expressing cells, green) from 5 roots for each condition. Scale bar, 20 μm.

(D) Seedlings from the indicated genotypes were inoculated with either WT or *ΔysnE* bacteria for 48 h on agar plates, and the number of colonizing bacteria was counted. Shown are averages and SD of at least two independent replicates (log_{10} transformed), with n = 3 for each, each circle represents an average of 3 technical replicates from the same root. (***$p < 0.005$, two-tailed t test with Bonferroni correction).

superoxide (O_2^-) ions, which can further be converted into other ROS, such as H_2O_2 (Wang et al., 2018). O_2^- was highly toxic to *B. velezensis in vitro* (Figure 4A), whereas H_2O_2 killed bacteria only at a high concentration (500 μM) (Figure S3E). O_2^- was significantly less toxic to WT bacteria in comparison with auxin-deficient bacteria (Figure 4A). Exogenous IAA enhanced the survival of both bacteria (Figure 4A). These results suggest that auxin enables bacteria to survive the toxic effects of ROS.

To gain a deeper understanding of the effect of auxin on bacterial interaction with ROS, we examined global gene expression changes in WT and *ΔysnE* bacteria in culture after the addition of O_2^-. In WT bacteria, 371 genes were upregulated and 374 genes downregulated (Figure 4B), whereas *ΔysnE* bacteria exhibited a weaker response (Figures 4B and 4C), with only 153 genes upregulated and 184 downregulated (Figure 4B; Table S3). Enriched GO categories for upregulated genes in WT bacteria included SOS response and DNA repair, whereas the DNA repair category was missing in *ΔysnE* (Figure 4D; Table S4). The *katA* and *ahpF* genes are important for ROS detoxification (Engelmann and Hecker, 1996; Poole, 2005), and the *recA* gene is important for DNA repair (Alonso et al., 2013). All three were upregulated in response to ROS treatment (Table S3, all three were induced to a greater extent in WT bacteria.). The expression of these genes in *ΔysnE* bacteria under an IPTG-inducible promoter significantly enhanced root colonization (Figure 4E). Interestingly, GO categories related to iron homeostasis were enriched in the transcriptome of WT bacteria but not in *ΔysnE* bacteria (Figure 4D and Table S4). Ferrous (Fe^{2+}) iron is known to interact with hydrogen peroxide in a Fenton reaction to produce a toxic hydroxyl radical (Cornelis et al., 2011), potentially amplifying the toxicity of the short-lived O_2^- molecules. Thus, iron sequestration can protect cells from the toxic effects of ROS. The expression of the siderophore bacillibactin or heme synthesis operons in *ΔysnE* bacteria under IPTG-inducible promoters enhanced their ability to colonize the root (Figure S4A). Lowering the iron content of MS media by 50% also improved root colonization by *ΔysnE* bacteria (Figure S4B). Of note, auxin was able to protect *B. velezensis* from iron toxicity *in vitro* (Figures S4C and S4D). Among the significantly depleted gene categories in WT bacteria were the TCA cycle and carbohydrate and amino acid transport, although none of these categories was depleted in *ΔysnE* bacteria (Table S4). We speculate that WT bacteria enter a growth arrest that can protect them from ROS toxicity, whereas *ΔysnE* bacteria that fail to induce growth arrest are killed. Thus, our results establish ROS as a major limiting factor during root colonization and auxin as a key bacterial effector to mitigate ROS toxicity. The addition of IAA to bacteria without ROS had negligible effects on transcription (Table S3), suggesting that auxin alone is not sufficient to explain these transcriptional changes and that other factors induced during stress are necessary for auxin to have its effect.

Given our findings that auxin plays a major role in mitigating ROS toxicity, we hypothesized that ROS exposure leads to auxin accumulation in bacteria. To test this hypothesis, we fused YsnE to GFP and observed that it accumulated upon ROS treatment *in vitro* (Figures S4E and S4F). We collected the supernatant from bacterial cultures treated with ROS and applied it to DR5::GFP-expressing plants, which led to a greater increase in DR5::GFP fluorescence as compared with plants treated with the supernatant from *ΔysnE* bacteria or from untreated WT bacteria (Figure 4F). Consistent with these results, *efr2* roots colonized by bacteria failed to exhibit

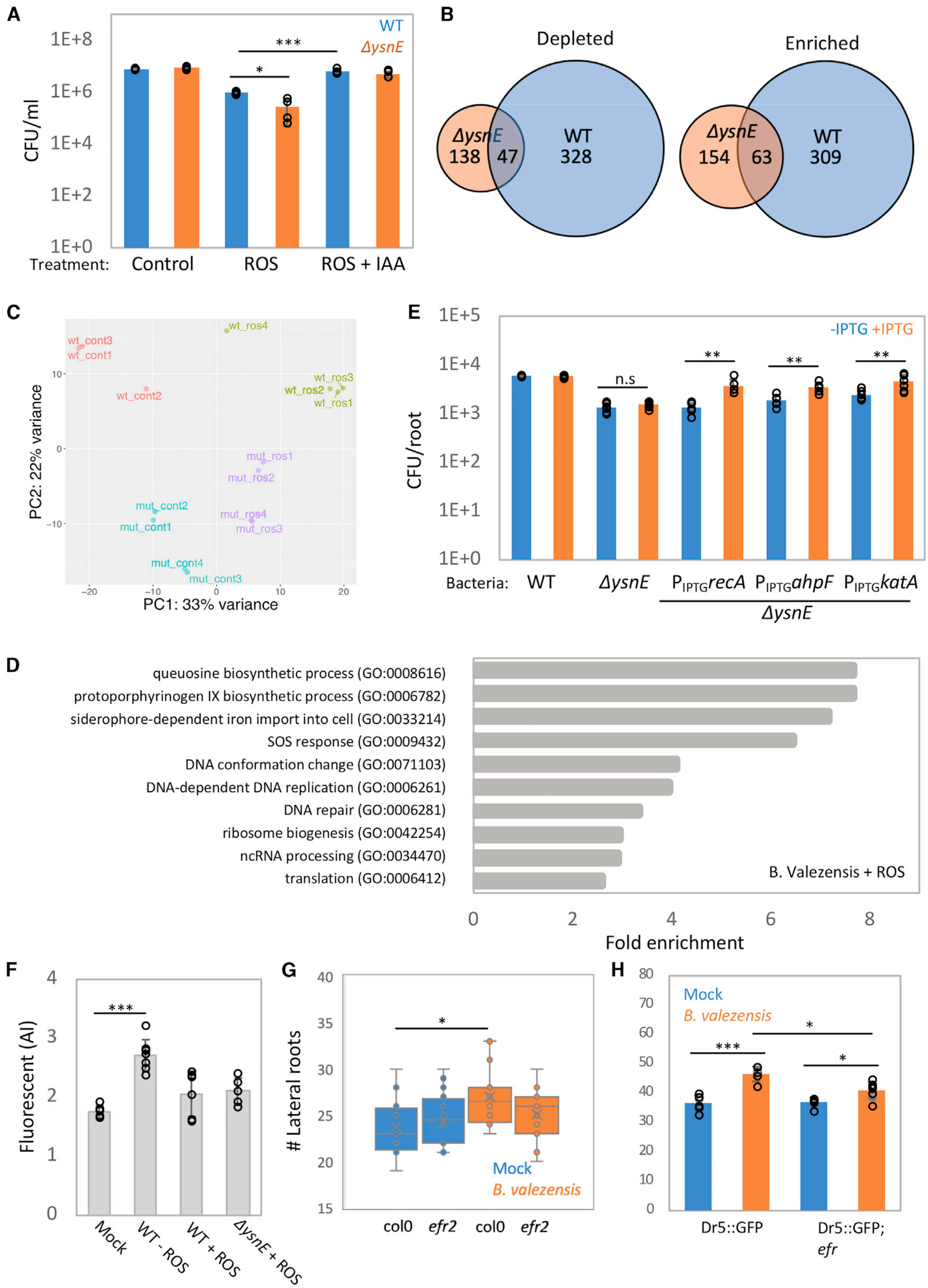

Figure 4. Bacterial auxin counteracts ROS toxicity

(A) Bacterial cultures grown to OD_{600} = 1 were treated with O_2^- in the presence or absence of 5 μM IAA for 30 min, and CFU were counted. Shown are averages and SD (log_{10} transformed) n = 3. Each circle represents an average of 3 technical replicates from the same culture. (*p < 0.05, ***p < 0.005, two-tailed t test with Bonferroni correction).

(legend continued on next page)

lateral root stimulation and had normal primary root length (Figures 4G and S4G). Furthermore, bacteria colonizing *efr2* plants harboring DR5::GFP induced significantly less GFP expression than DR5::GFP WT plants (Figure 4H), suggesting that EFR-induced ROS production by the plant is necessary to trigger efficient bacterial auxin production.

Auxin promotes bacterial adhesion and colony formation on the root

Although the growth of *ΔysnE* bacteria is restored on *efr2* roots (Figures 2E and S2C), these bacteria do not adhere to the root in the same way in which WT bacteria adhere to Col-0 roots (Figure 3A). Interestingly, similar inefficient adhesion occurred when WT bacteria colonized *efr2* roots (Figures 5A, 5B, S5A, and S5B). The quantification of root adhesion from time-lapse microscopy revealed that, on average, 83% of bacteria colonizing WT Col-0 roots remained adhered to the root during a 12-h experiment (Figure 5A), while only 32% did so on *efr2* roots (Figures 5A and S5A). The macrostructure of bacteria colonizing a root after 48 h revealed large clusters on Col-0 roots (Figures 5B and S5B), while bacteria colonizing *efr2* roots were in small patches (Figures 5B and S5B), probably reflecting the same phenomenon of perturbed adhesion and colony formation. This suggests that efficient ROS response, perturbed in *efr2* roots, is necessary for tight root adhesion and colony formation. The addition of exogenous IAA stimulated colonization on Col-0 as well as on *efr2* plants (Figure 5C). Exogenous IAA can stimulate root colonization on mutant plants impaired in auxin perception (Figures S5C and S5D), suggesting that auxin, at least in part, affects the bacterial ability to adhere to the root rather than the root's response to bacteria, although root response cannot be excluded.

To elucidate the mechanism by which auxin promotes root adhesion and spreading, we screened an array of colonization-related mutant bacteria, impaired in motility, adhesion, and biofilm formation genes (Chen et al., 2007), for auxin-enhanced colonization (Figure 5D). Bacteria with a mutated lipoteichoic-acid synthase gene, Δ*yfnI*, lost their ability to colonize the root, irrespective of IAA addition. Bacteria lacking a flagellar apparatus, Δ*hag*, colonized the roots similar to WT bacteria. However, they failed to exhibit enhanced colonization following IAA addition (Figures 5C and 5D). Auxin-induced flagellar formation was also suggested by the transcriptome analysis (Table S3, IAA-induced *hag* gene expression logFC = 0.79) and *in vitro* motility assay (Figure S5E). Δ*hag* bacteria also failed to induce lateral root formation (Figure 5E). Interestingly, similar results were obtained with Δ*swrA* bacteria, a regulator of flagellar synthesis. However, Δ*motA* bacteria, harboring intact but nonmotile flagella, were still able to respond to IAA addition (Figure S5F), suggesting that the presence of flagella, but not its movement, is what is important for root adhesion. We conclude that auxin-induced flagella production is able to enhance root colonization necessary for lateral root stimulation.

The plant immune system stimulates root colonization and auxin secretion by diverse bacterial species

To determine if bacterial auxin secretion and plant immunity interact in a similar manner for other bacteria, we analyzed the colonization capacity of *Paenibacillus polymyxa* (*P. polymyxa*), a Gram-positive bacteria known to secrete high amounts of auxin and stimulate plant growth (Jeong et al., 2011). *P. polymyxa* stimulated lateral root formation, shorter primary roots, and DR5::GFP expression in roots on agar plates (Figures 6A–6C). *P. polymyxa* also stimulated plant ROS production in an FLS2-dependent manner (Figure 6D). On *fls2* plants, *P. polymyxa* failed to stimulate lateral root production (Figure 6B) and had longer primary roots as compared with Col-0 (Figure 6C), despite the bacteria reaching a higher CFU on *fls2* plants (Figure 6E), suggesting that immune system activation and ROS production are necessary for bacterial auxin production. Furthermore, exogenous IAA stimulated root colonization by *P. polymyxa* (Figure 6F). Finally, IAA induced FLS promoter expression (Figure 6G). Thus, auxin produced by *P. polymyxa* and plant immunity interact with each other, despite being modulated by a different immune receptor than *B. velezensis*. *Arthrobacter MF161* is another Gram-positive auxin-secreting bacterium isolated from Arabidopsis roots (Levy et al., 2017). Inoculation by this bacterial strain stimulated lateral root formation and DR5::GFP expression (Figures S6A and S6B), as well as triggering the immune response in an FLS2-dependent manner (Figure S6C). *Arthrobacter MF161* failed to enhance lateral root formation and had longer primary roots on *fls2* plants (Figures S6B and S6D). No difference in root colonization was observed between Col-0 and *fls2* plants (Figure S6E) Finally, exogenous IAA further stimulated root colonization by this bacterial strain (Figure S6F). Auxin did not stimulate root colonization of auxin-secreting *Pseudomonas* species *65* (Kamilova et al., 2006) and *WCS374* (Zamioudis et al., 2013) (Figure S6G), suggesting

(B) Venn diagram illustrating significantly affected genes. On the left are genes depleted after O_2^- treatment, on the right genes enriched after O_2^- treatment.

(C) Principal component analysis of RNA sequenced from WT or *ΔysnE* bacteria treated with O_2^- at a sub-lethal concentration (see Figure S3F) for 30 min or with the substrate alone as a control.

(D) Representative biological processes GO term analysis of genes upregulated in response to O_2^- treatment. $p < 0.05$. (See Table S4 for the full list of GO categories).

(E) Seedlings were inoculated with the indicated bacterial strains on plates containing 0.5 mM IPTG (+IPTG) or in the absence of IPTG (−IPTG) for 48 h and the number of colonizing bacteria was counted. Shown are averages and SD of 2 independent experiments (log_{10} transformed), with $n \geq 3$ for each, each circle represents an average of 3 technical replicates from the same root. (**$p < 0.01$, two-tailed t test).

(F) Arabidopsis DR5::GFP reporter lines were inoculated for 12 h with media derived from WT or *ΔysnE* bacteria grown to $OD_{600} = 1$ and treated with O_2^- for 30 min. Shown are average and SD of fluorescent intensity from DR5::GFP, ($n \geq 5$), each circle represents one root. (***$p < 0.005$, two-tailed t test with Bonferroni correction).

(G) Seedlings of Col-0 or *efr2* plants were inoculated with bacteria or buffer (mock) on agar plates for 7 days and the number of lateral roots was counted. ($n \geq 20$) (*$p < 0.05$, ANOVA followed by post hoc Tukey Kramer).

(H) Arabidopsis DR5::GFP reporter lines, and *efr2*; DR5::GFP were inoculated with the indicated bacterial strains for 48 h on agar plates and GFP fluorescence quantified from maximum intensity projection images. Shown are average and SD n = 5, each circle represents one root. (*$p < 0.05$, ***$p < 0.005$, two-tailed t test with Bonferroni correction).

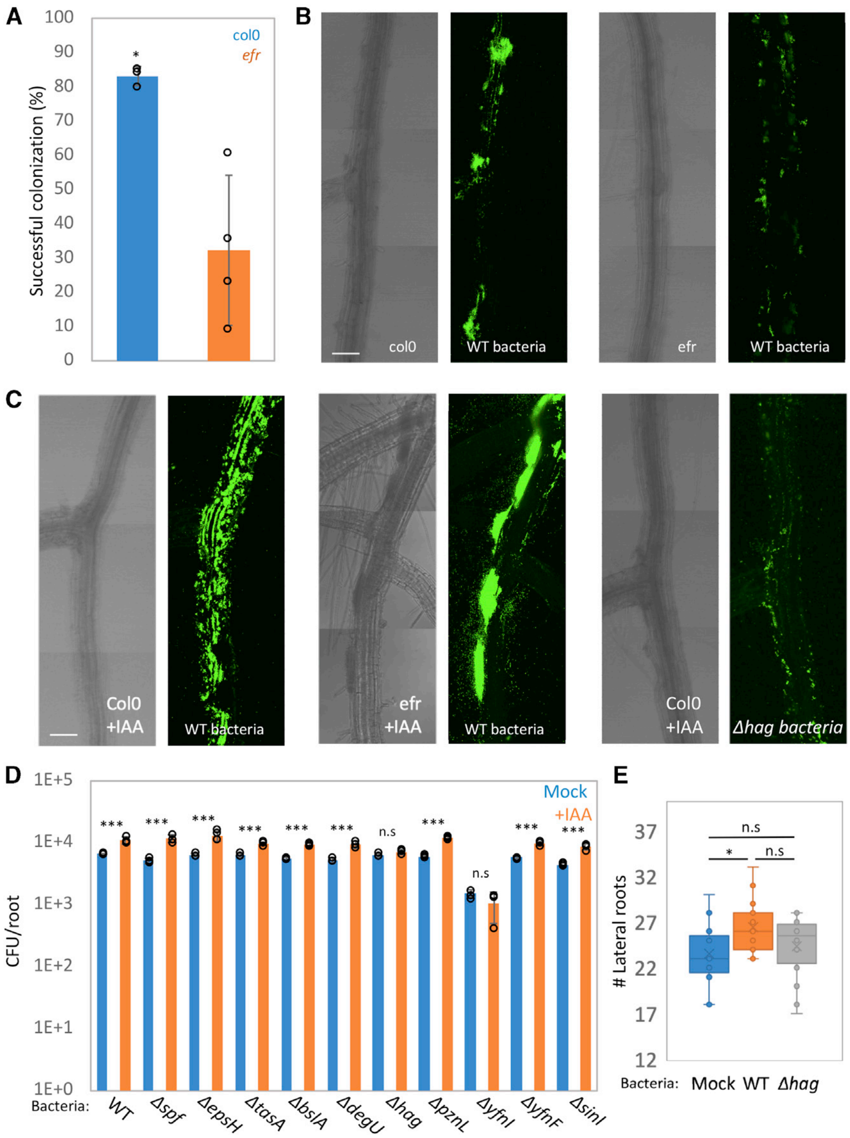

Figure 5. ROS induces auxin-enhanced root colonization through the stimulation of bacterial flagella

(A) Col-0 or *efr2* seedlings were inoculated with GFP-expressing bacteria (*amyE::Pspac-gfp*) and followed by time-lapse confocal microscopy for 12 h. Spots of colonizing bacteria were counted at t = 2 h and followed until t = 12 h. Bacteria remaining attached during this time course were counted as successful colonization events (see an example in Figure S6A). Shown are percentages of successful colonization at t = 12 h of total spots of colonizing bacteria at t = 2 h. The results are averages and SD from at least 3 time-lapse experiments for each genotype. n $\geq$ 25 spots for each time lapse, each circle represents one time lapse experiment. (*p < 0.05, two-tailed t test).

(B and C) Seedlings were inoculated with the indicated bacterial strains expressing GFP, for 48 h on agar plates. In the absence (B) or presence of 5 μM IAA (C). Shown are 200$\times$ maximal projection confocal images of DIC from roots (left panels) and GFP fluorescence from bacteria (right panels). Scale bars, 50 μm.

(D) Seedlings were inoculated with the indicated bacterial strains with or without 5 μM IAA for 48 h on agar plates and the number of colonizing bacteria was counted. Shown are averages and SD ($\log_{10}$ transformed), n = 3, each circle represents an average of three technical replicates from the same root. (***p < 0.005, two-tailed t test with Bonferroni correction).

(E) Seedlings were inoculated with either WT or *Δhag* bacteria or buffer alone (mock) on agar plates for 7 days and the number of lateral roots was counted. n $\geq$ 20, (*p < 0.05, ANOVA followed by post hoc Tukey Kramer).

that auxin-stimulated colonization is not a general phenomenon but is bacterium specific.

Our results indicate that ROS production by the plant immune system is necessary for efficient root adhesion. However, this phenomenon is not manifested in differences in bacterial load (Figure 5). Given that bacteria in nature compete with many other species to inhabit the same plant root niche (Bai et al., 2015; Lundberg et al., 2012), we hypothesized that differences in *B. velezensis* root adhesion ability would become evident during competition with other bacteria. To test this hypothesis, we co-inoculated *P. polymyxa* and *B. velezensis* on Col-0 and *efr2* plants. *P. polymyxa* colonization was only modulated by the FLS receptor but not by EFR (Figure 6D), whereas *B. velezensis* colonization was mainly modulated by the EFR receptor (Figure 2D). After co-inoculation, *B. velezensis* outcompeted *P. polymyxa* on Col-0 (Figure 6H). However, on *efr2* plants, we observed a significant increase in *P. polymyxa* colonization, concomitant with a reduction of *B. velezensis* colonization (Figure 6H). *B. velezensis* inoculated onto Col-0 and *efr2* plants for 48 h and then transferred into nonsterile soil also exhibited enhanced colonization of Col-0 plants (Figure 6I), indicating that immune modulation helps the bacteria to compete with the soil microbiota. Co-inoculation of *B. velezensis* and *Arthrobacter MF161* on Col-0 and *efr2* plants had no significant effect on either bacteria (Figure S7A). The inspection of colonization sites revealed that *B. velezensis* and *P. polymyxa* heavily colonize the elongation and maturation zones of the root (Figures S7B1 and S7B2), whereas *Arthrobacter MF161* is largely absent from these regions and colonizes differentiated parts of the root (Figures S7B3 and S7B4). Thus, our results suggest that immune system enhanced colonization affects *B. velezensis* and *P. polymyxa* competition, as both compete for the same niche, but not *B. velezensis* and *Arthrobacter MF61* competition, as they colonize different niches. Root colonization by *Arthrobacter MF161* inside a synthetic community of 34 bacteria was previously characterized (Castrillo et al., 2017; Teixeira et al., 2021). To explore the possibility that immune modulation of *Arthrobacter MF161* by FLS affects its root colonization inside the community, we performed 16S RNA sequencing of the 34 bacterial community, colonizing

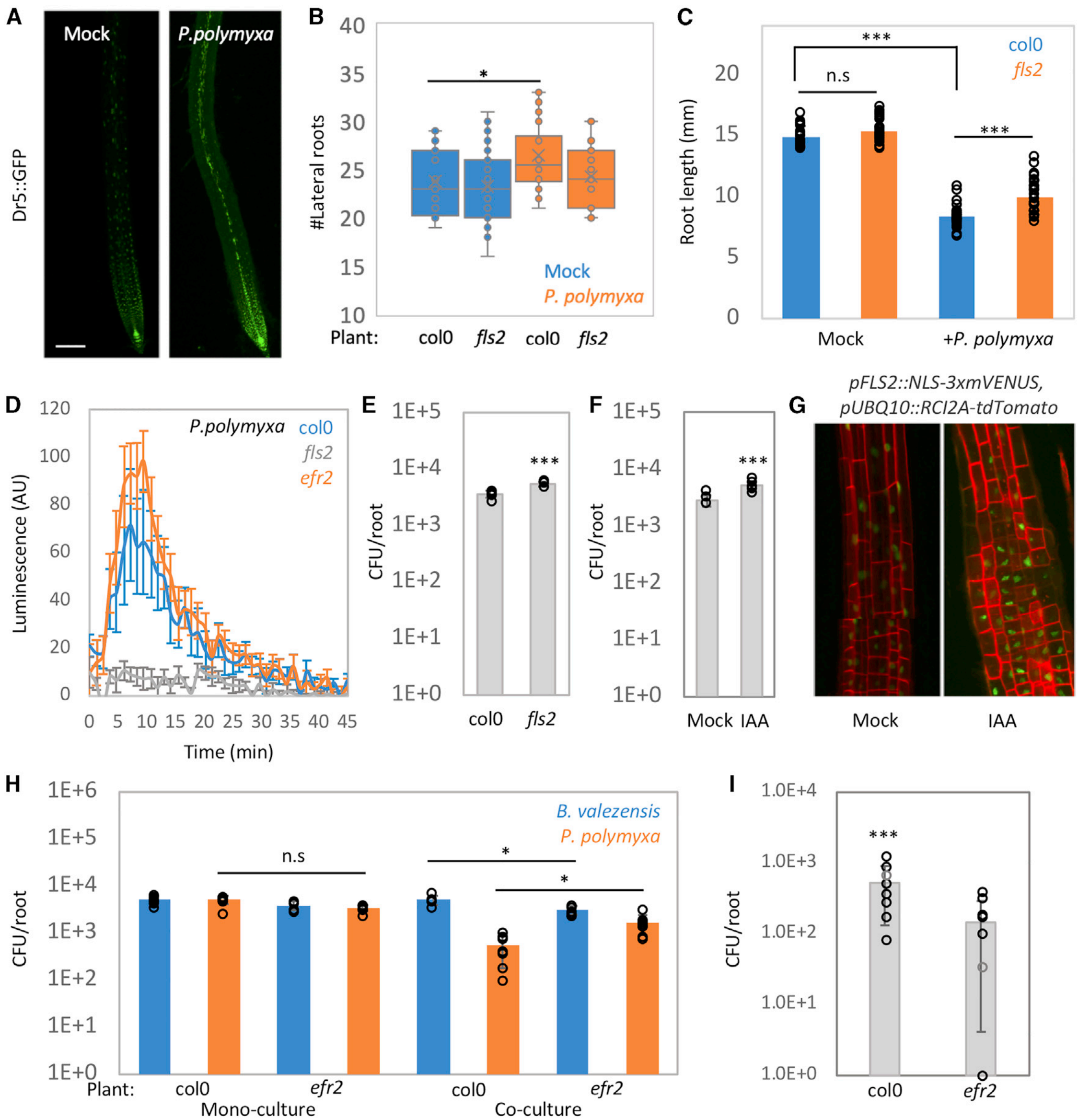

Figure 6. Plant immunity interaction with bacterial auxin secretion in *P. polymyxa*

(A) An Arabidopsis DR5::GFP reporter line was inoculated with *P. polymyxa* for 96 h on agar plates. Shown are 100× maximal projection confocal images of GFP fluorescence from the DR5::GFP reporter line.

(B) Col-0 or *fls2* seedlings were inoculated with *P. polymyxa* or buffer (mock) on agar plates for 7 days and the number of lateral roots was counted, $n \geq 20$. (*$p < 0.05$, ANOVA followed by post hoc Tukey Kramer).

(C) Col-0 or *fls2* seedlings were inoculated with *P. polymyxa* or buffer alone (mock) on agar plates for 7 days and the length of the primary root was measured, $n \geq 20$. Each circle represents one root. (***$p < 0.005$, two-tailed t test with Bonferroni correction).

(D) Leaf discs from 28-day-old plants taken from the indicated plant genotypes were incubated with bacteria adjusted to OD 0.1, and the ROS burst was measured. Shown are averages and SD, $n \geq 10$.

(E) Col-0 or *fls2* seedlings were inoculated with *P. polymyxa* for 48 h on agar plates and the number of colonizing bacteria was counted. Shown is an average and SD of two independent replicates ($\log_{10}$ transformed), with n = 3 for each. Each circle represents an average of 3 technical replicates from the same root. (***$p < 0.005$, two-tailed t test).

(F) Seedlings were inoculated with *P. polymyxa* for 48 h on agar plates with or without 5 μM IAA and the number of colonizing bacteria was counted. Shown are averages and SD of 2 independent replicates ($\log_{10}$ transformed), with n = 3 for each. Each circle represents an average of 3 technical replicates from the same root. (***$p < 0.005$, two-tailed t test).

(G) Seedlings of *pFLS::NLS-3xmVENUS, pUBQ10::RCI2A-tdTomato* were inoculated with WT bacteria, grown in the presence of 5 μM IAA, or buffer for 48 h. Shown are 400× representative overlay images of *pUBQ10::RCI2A-tdTomato* (cell wall, red) and *pFLS::NLS-3xmVENUS* (FLS-expressing cells, green) from five roots for each condition. Scale bar, 25 μm.

(legend continued on next page)

either Col-0 or *fls2* plants. However, the results were inconclusive (Figure S7C), suggesting that the community context is important for *Arthrobacter* colonization.

B. velezensis produces secondary metabolites that can inhibit the growth of plant fungal pathogens (Fan et al., 2018). We asked if plant immune system activation, triggering *B. velezensis* colony formation, enhances its ability to inhibit plant pathogen infection. We colonized Col-0 and *efr2* plants with *B. velezensis* and infected the plants with the fungal pathogen *Rhizoctonia solani* (Dean et al., 2012). *B. velezensis* inhibits the growth of *R. solani in vitro* (Figure 7A) and is able to protect plants from fungal infection (Figure 7B) (Chowdhury et al., 2013). Of note, plant protection was significantly better on Col-0 plants, as measured by plant weight, although *efr2* has no effect on fungal infection per se, (Figure 7C *R. solani* alone). Monitoring the fungal load reveals a significant reduction on Col-0 plants in comparison with *efr2* plants (Figure 7D). EFR activation modulates *B. velezensis* colony formation but may also enhance plant survival through induced systemic resistance (ISR) (Pieterse et al., 2014). To further differentiate between these effects, we measured plant protection by Δ*hag B. velezensis* (Figure 7C). Δ*hag* bacteria failed to protect the seedlings from *R. solani* infection (Figure 7C), despite inducing an immune response in the plant, similar to WT bacteria (Figure 7E). Thus, we conclude that the enhanced colony formation of *B. velezensis* on immune competent plants enables it to better protect the plant from fungal infection.

DISCUSSION

Our results are consistent with the presence of a feedback loop between the plant immune system and bacterial auxin secretion (Figure 7F). Root colonization by bacteria triggers an immune response and ROS production. ROS, in turn, elicits bacterial auxin production to mitigate ROS toxicity. Auxin promotes bacterial spreading over the root and colony formation, while also inducing the expression of plant immune receptors, further accelerating the feedback loop. This enhanced colonization promotes the ability of *B. velezensis* to inhibit plant pathogenic fungi. Thus, a feedback loop between bacteria and the plant immune system promotes the fitness of both partners.

Recent work has elucidated the role of the plant immune system in shaping the normal root microbiota, in addition to fighting pathogens (Hacquard et al., 2017; Teixeira et al., 2019). In these studies, an immune reaction was viewed as a negative factor for root colonization, shaping the microbiota by preventing bacterial overgrowth. Consistent with this view, our results show that *B. velezensis* modestly overgrows on *rbohd rbohf* plants completely lacking ROS production (Figure 3D). However, bacteria grow on *efr2* plants with partially perturbed immunity, demonstrating that plant immune system activation also plays a positive role for bacterial colonization, triggering the induction of auxin production by bacteria necessary for efficient root adhesion and colony formation. We hypothesize that bacteria exhibit significantly higher growth on *rbohd rbohf* but not *efr* plants due to the fact that ROS is still produced in *efr2* plants (Figure 2B), probably through activation of other immune receptors. Consistently, bacteria overgrew *bak1-5* plants, defective in the activation of multiple receptors (Figure S3A). In addition, *rbohd rbohf* plants also exhibit non-immune-related phenotypes that may affect bacterial colonization (e.g., Song et al., 2021).

Our results suggest that immune system activation interacts with bacterial auxin secretion to enhance bacterial colonization, irrespective of the specific immune receptor, as we provide evidence that a similar feedback loop exists during *P. polymyxa* and *Arthrobacter MF161* colonization, despite being modulated by the FLS2 receptor rather than the EFR2 receptor. Thus, we uncovered a unique aspect of bacterial interaction with the immune system.

A prevalent view of mutualistic interactions is that symbiosis evolved through exploitative interactions that became attenuated over evolutionary time (Cao et al., 2017; Delaux and Schornack, 2021; Sachs et al., 2011). Parallels were found between the immune system signaling pathway and the symbiotic association between plants and specialized mutualists, such as the interaction between legumes and rhizobia (Cao et al., 2017; Tóth and Stacey, 2015), as well as the association between plants and arbuscular mycorrhizal fungi (Miyata et al., 2014). Our results reveal a more widespread relationship between plant immunity and colonization of beneficial bacteria, including nonspecialized auxin-secreting beneficial bacteria, potentially representing an earlier stage of the evolution of mutualism.

Auxin is a key plant hormone that plays a wide range of roles in plant development (Teale et al., 2006). Many bacterial species, including pathogens such as *Agrobacterium tumefaciens* and *Pseudomonas syringae*, as well as beneficial bacteria such as *Azospirillum brasilense*, are known to synthesize auxin and manipulate the plant through auxin secretion (Costacurta and Vanderleyden, 1995; Kunkel and Harper, 2018; Spaepen et al., 2007). However, despite decades of research on bacterial auxin production and how it affects plants, the role played by auxin on bacterial physiology is poorly understood. Previous studies found a bacterial transcriptional effect for auxin, but only at concentrations far above those that modify plant physiology (Bianco et al., 2006; Djami-Tchatchou et al., 2020; Van Puyvelde et al., 2011). Our results suggest that auxin primarily affects the producer bacteria, acting as a stress-related signal to protect them from ROS. Mutations in the auxin synthesis pathway lead to profound transcriptional effects following ROS treatment. However, we failed to observe a substantial role for exogenous IAA under nonstressed conditions. This suggests that auxin may not be sufficient by itself to induce a significant response in bacteria similar to its effect on plants. Rather, auxin needs other factors that are induced during stress to have its effect. Further research will be necessary to elucidate the role played

(H) Seedlings were inoculated with either *P. polymyxa* or *B. velezensis* alone (monoculture) or in a mixture (1:1 ratio, co-culture) for 48 h on agar plates and the number of colonizing bacteria from each strain was counted. Shown are averages and SD of 2 independent replicates ($\log_{10}$ transformed), with n = 3 for each. Each circle represents an average of 3 technical replicates from the same root. (*p < 0.05, two-tailed t test with Bonferroni correction).

(I) Col-0 or *efr2* seedlings were inoculated with *B. velezensis* for 48 h on agar plates, and then the seedlings were transferred to nonsterile potting soil for 7 days and the number of colonizing *B. velezensis* was counted. Shown is an average and SD ($\log_{10}$ transformed), n = 8. Each circle represents an average of three technical replicates from the same root. (***p < 0.005, two-tailed t test).

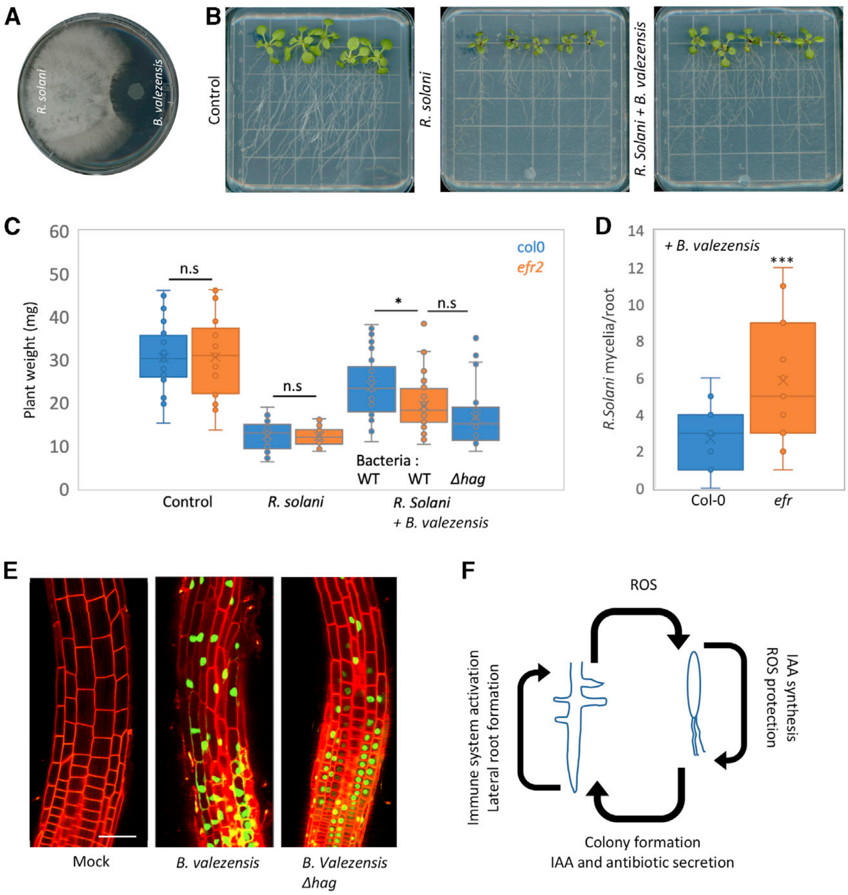

Figure 7. Immune system modulation by *B. velezensis* enhances plant protection from fungal infection

(A) *B. velezensis* and *R. solani* were spotted on PDA plates and allowed to grow for 72 h. Shown is a representative plate from 3 plates.

(B) 6-day-old seedlings were inoculated with *B. velezensis* or buffer for 48 h on agar plates. Then, the plates were inoculated with *R. solani* and incubated for an additional 7 days. Untreated plants were used as a control. Shown are representative plates from at least 5 plates for each treatment.

(C) Col-0 or *efr2* seedlings were inoculated with WT or *Δhag* (only Col-0) *B. velezensis*, or buffer for 48 h on agar plates. Then, the plates were inoculated with *R. solani* and incubated for an additional 7 days and plant weight was measured. Untreated plants (neither bacteria nor fungi) were used as a control. Shown are averages and SD, n $\geq$ 20. (*$p < 0.05$, two-tailed t test with Bonferroni correction).

(D) 6-day-old seedlings were inoculated with *B. velezensis* or buffer for 48 h on agar plates. Then, the plates were inoculated with *R. solani* and incubated for an additional 3 days. After 3 days, seedlings were thoroughly washed and transferred to new plates and the number of attached mycelia were counted under the microscope after 24 h. Control plants were completely covered by fungi, precluding detailed quantification. (***$p < 0.005$ two-tailed t test).

(E) *pPER5::NLS-3xmVENUS*, *pUBQ10::RCI2A-tdTomato* seedlings were inoculated with either WT or *Δhag B. velezensis* or buffer alone (mock) for 48 h. Shown are 400× overlay images of *pUBQ10::RCI2A-tdTomato* (red) and *pPER5::NLS-3xmVENUS* (green) from 5 roots from each condition. Scale bars, 25 μm.

(F) Model describing the feedback loop between plant immune system activation and bacterial auxin secretion.

by auxin in bacterial physiology and stress adaptation for beneficial, as well as pathogenic bacteria.

Plants interact with a wide variety of bacterial species in nature. The composition of the plant microbiome is affected by factors such as soil geochemistry, bacterial diversity, the amount and composition of exudates, immune system activation, and by bacterial interaction with other bacteria, with phages, and with other organisms. Understanding the effect of each of these components will enable rational manipulation of the plant microbiome to the benefit of the plant. Bacterial auxin production is highly prevalent among root-colonizing bacteria (Zhang et al., 2019), and the effect of auxin-secreting and -degrading bacteria in the root microbiome on plant physiology in a complex microbiome was recently explored (Finkel et al., 2020). Here, we have shown that auxin-secreting bacteria interact with the plant immune system to promote their association with the plant and their competition with other bacteria.

STAR★METHODS

Detailed methods are provided in the online version of this paper and include the following:

- KEY RESOURCES TABLE
- RESOURCE AVAILABILITY
  - Lead contact
  - Materials availability
  - Data and code availability
- EXPERIMENTAL MODEL AND SUBJECT DETAILS
  - Bacteria
  - Fungi
  - Plants
- METHOD DETAILS
  - Bacterial genetic manipulation
  - Monitoring bacterial growth on plant roots
  - Microscopy
  - Measurement of plant ROS production
  - RNA extraction library preparation and computational analysis
- QUANTIFICATION AND STATISTICAL ANALYSIS

SUPPLEMENTAL INFORMATION

Supplemental information can be found online at https://doi.org/10.1016/j.chom.2021.09.005.

ACKNOWLEDGMENTS

We thank G. Wachsman for help in RNA sequence analysis. We are grateful to S.Y He (Duke), X. Dong (Duke), B. Kunkel (Washington University), T. Nolan, R. Shahan, and C. Winter from the Benfey lab, for critical reading of the manuscript. Funding: this work was supported by a grant from the NSF (NSF PHY-1915445) to P.N.B., by the Howard Hughes Medical Institute to P.N.B., and by a BARD Post-doctoral fellowship (FI-574-2018) to E.T. This work was supported by the NSF grant IOS-1917270 to J.L.D.; J.L.D. is an investigator at the Howard Hughes Medical Institute, supported by the HHMI. D.R. is supported by EMBO Long Term Fellowship (ALTF 743–2019).

AUTHOR CONTRIBUTIONS

E.T. and P.N.B. conceived the project. E.T. performed the experiments. D.R. designed and analyzed experiments. J.L.D. donated strains. E.T. wrote an initial draft. P.N.B., J.L.D., and D.R. reviewed and edited the manuscript.

DECLARATION OF INTERESTS

The authors declare no competing interests.

Received: April 7, 2021
Revised: July 7, 2021
Accepted: August 24, 2021
Published: October 4, 2021

REFERENCES

Alonso, J.C., Cardenas, P.P., Sanchez, H., Hejna, J., Suzuki, Y., and Takeyasu, K. (2013). Early steps of double-strand break repair in Bacillus subtilis. DNA Repair (Amst) *12*, 162–176.

Bai, Y., Müller, D.B., Srinivas, G., Garrido-Oter, R., Potthoff, E., Rott, M., Dombrowski, N., Münch, P.C., Spaepen, S., Remus-Emsermann, M., et al. (2015). Functional overlap of the Arabidopsis leaf and root microbiota. Nature *528*, 364–369.

Banda, J., Bellande, K., von Wangenheim, D., Goh, T., Guyomarc'h, S., Laplaze, L., and Bennett, M.J. (2019). Lateral root formation in Arabidopsis: a well-ordered LRexit. Trends Plant Sci *24*, 826–839.

Bianco, C., Imperlini, E., Calogero, R., Senatore, B., Amoresano, A., Carpentieri, A., Pucci, P., and Defez, R. (2006). Indole-3-acetic acid improves Escherichia coli's defences to stress. Arch. Microbiol. *185*, 373–382.

Branda, S.S., González-Pastor, J.E., Ben-Yehuda, S., Losick, R., and Kolter, R. (2001). Fruiting body formation by Bacillus subtilis. Proc. Natl. Acad. Sci. USA *98*, 11621–11626.

Bray, N.L., Pimentel, H., Melsted, P., and Pachter, L. (2016). Near-optimal probabilistic RNA-seq quantification. Nat. Biotechnol. *34*, 525–527.

Callahan, B.J., McMurdie, P.J., Rosen, M.J., Han, A.W., Johnson, A.J., and Holmes, S.P. (2016). DADA2: high-resolution sample inference from Illumina amplicon data. Nat. Methods *13*, 581–583.

Cao, Y., Halane, M.K., Gassmann, W., and Stacey, G. (2017). The role of plant innate immunity in the legume-rhizobium symbiosis. Annu. Rev. Plant Biol. *68*, 535–561.

Castrillo, G., Teixeira, P.J., Paredes, S.H., Law, T.F., de Lorenzo, L., Feltcher, M.E., Finkel, O.M., Breakfield, N.W., Mieczkowski, P., Jones, C.D., et al. (2017). Root microbiota drive direct integration of phosphate stress and immunity. Nature *543*, 513–518.

Chen, T., Nomura, K., Wang, X., Sohrabi, R., Xu, J., Yao, L., Paasch, B.C., Ma, L., Kremer, J., Cheng, Y., et al. (2020). A plant genetic network for preventing dysbiosis in the phyllosphere. Nature *580*, 653–657.

Chen, X.H., Koumoutsi, A., Scholz, R., Eisenreich, A., Schneider, K., Heinemeyer, I., Morgenstern, B., Voss, B., Hess, W.R., Reva, O., et al. (2007). Comparative analysis of the complete genome sequence of the plant growth-promoting bacterium Bacillus amyloliquefaciens FZB42. Nat. Biotechnol. *25*, 1007–1014.

Chen, Y., Yan, F., Chai, Y., Liu, H., Kolter, R., Losick, R., and Guo, J.H. (2013). Biocontrol of tomato wilt disease by Bacillus subtilis isolates from natural environments depends on conserved genes mediating biofilm formation. Environ. Microbiol. *15*, 848–864.

Chowdhury, S.P., Dietel, K., Rändler, M., Schmid, M., Junge, H., Borriss, R., Hartmann, A., and Grosch, R. (2013). Effects of Bacillus amyloliquefaciens FZB42 on lettuce growth and health under pathogen pressure and its impact on the rhizosphere bacterial community. PLoS One *8*, e68818.

Chowdhury, S.P., Uhl, J., Grosch, R., Alquéres, S., Pittroff, S., Dietel, K., Schmitt-Kopplin, P., Borriss, R., and Hartmann, A. (2015). Cyclic lipopeptides of Bacillus amyloliquefaciens subsp. plantarum colonizing the lettuce rhizosphere enhance plant defense responses Toward the bottom rot pathogen Rhizoctonia solani. Mol. Plant Microbe Interact. *28*, 984–995.

Colaianni, N.R., Parys, K., Lee, H.S., Conway, J.M., Kim, N.H., Edelbacher, N., Mucyn, T.S., Madalinski, M., Law, T.F., Jones, C.D., et al. (2021). A complex immune response to flagellin epitope variation in commensal communities. Cell Host Microbe *29*, 635–649, e9.

Cornelis, P., Wei, Q., Andrews, S.C., and Vinckx, T. (2011). Iron homeostasis and management of oxidative stress response in bacteria. Metallomics *3*, 540–549.

Costacurta, A., and Vanderleyden, J. (1995). Synthesis of phytohormones by plant-associated bacteria. Crit. Rev. Microbiol. *21*, 1–18.

Couto, D., and Zipfel, C. (2016). Regulation of pattern recognition receptor signalling in plants. Nat. Rev. Immunol. *16*, 537–552.

Dean, R., Van Kan, J.A., Pretorius, Z.A., Hammond-Kosack, K.E., Di Pietro, A., Spanu, P.D., Rudd, J.J., Dickman, M., Kahmann, R., Ellis, J., and Foster, G.D. (2012). The Top 10 fungal pathogens in molecular plant pathology. Mol. Plant Pathol. *13*, 414–430.

Delaux, P.M., and Schornack, S. (2021). Plant evolution driven by interactions with symbiotic and pathogenic microbes. Science *371*.

Dietel, K., Beator, B., Budiharjo, A., Fan, B., and Borriss, R. (2013). Bacterial traits involved in colonization of Arabidopsis thaliana Roots by Bacillus amyloliquefaciens FZB42. Plant Pathol. J. *29*, 59–66.

Ding, P., and Ding, Y. (2020). Stories of salicylic acid: a plant defense hormone. Trends Plant Sci *25*, 549–565.

Djami-Tchatchou, A.T., Harrison, G.A., Harper, C.P., Wang, R., Prigge, M.J., Estelle, M., and Kunkel, B.N. (2020). Dual role of auxin in regulating plant defense and bacterial virulence gene expression during Pseudomonas syringae PtoDC3000 pathogenesis. Mol. Plant Microbe Interact. *33*, 1059–1071.

Dodds, P.N., and Rathjen, J.P. (2010). Plant immunity: towards an integrated view of plant-pathogen interactions. Nat. Rev. Genet. *11*, 539–548.

Duca, D., Lorv, J., Patten, C.L., Rose, D., and Glick, B.R. (2014). Indole-3-acetic acid in plant-microbe interactions. Antonie Leeuwenhoek *106*, 85–125.

Engelmann, S., and Hecker, M. (1996). Impaired oxidative stress resistance of Bacillus subtilis sigB mutants and the role of katA and katE. FEMS Microbiol. Lett. *145*, 63–69.

Fan, B., Chen, X.H., Budiharjo, A., Bleiss, W., Vater, J., and Borriss, R. (2011). Efficient colonization of plant roots by the plant growth promoting bacterium Bacillus amyloliquefaciens FZB42, engineered to express green fluorescent protein. J. Biotechnol. *151*, 303–311.

Fan, B., Wang, C., Song, X., Ding, X., Wu, L., Wu, H., Gao, X., and Borriss, R. (2018). *Bacillus velezensis* FZB42 in 2018: the Gram-positive model strain for plant growth promotion and biocontrol. Front. Microbiol. *9*, 2491.

Finkel, O.M., Salas-González, I., Castrillo, G., Conway, J.M., Law, T.F., Teixeira, P.J.P.L., Wilson, E.D., Fitzpatrick, C.R., Jones, C.D., and Dangl, J.L. (2020). A single bacterial genus maintains root growth in a complex microbiome. Nature *587*, 103–108.

Fones, H., and Preston, G.M. (2012). Reactive oxygen and oxidative stress tolerance in plant pathogenic Pseudomonas. FEMS Microbiol. Lett. *327*, 1–8.

Frerigmann, H., Berger, B., and Gigolashvili, T. (2014). bHLH05 is an interaction partner of MYB51 and a novel regulator of glucosinolate biosynthesis in Arabidopsis. Plant Physiol *166*, 349–369.

Gohl, D.M., Vangay, P., Garbe, J., MacLean, A., Hauge, A., Becker, A., Gould, T.J., Clayton, J.B., Johnson, T.J., Hunter, R., et al. (2016). Systematic improvement of amplicon marker gene methods for increased accuracy in microbiome studies. Nat. Biotechnol. *34*, 942–949.

Hacquard, S., Spaepen, S., Garrido-Oter, R., and Schulze-Lefert, P. (2017). Interplay Between innate immunity and the plant microbiota. Annu. Rev. Phytopathol. *55*, 565–589.

Idris, E.E., Iglesias, D.J., Talon, M., and Borriss, R. (2007). Tryptophan-dependent production of indole-3-acetic acid (IAA) affects level of plant growth promotion by Bacillus amyloliquefaciens FZB42. Mol. Plant Microbe Interact. *20*, 619–626.

Jeong, H., Park, S.Y., Chung, W.H., Kim, S.H., Kim, N., Park, S.H., and Kim, J.F. (2011). Draft genome sequence of the Paenibacillus polymyxa type strain (ATCC 842T), a plant growth-promoting bacterium. J. Bacteriol. *193*, 5026–5027.

Jones, J.D., and Dangl, J.L. (2006). The plant immune system. Nature *444*, 323–329.

Kamilova, F., Kravchenko, L.V., Shaposhnikov, A.I., Azarova, T., Makarova, N., and Lugtenberg, B. (2006). Organic acids, sugars, and L-tryptophane in exudates of vegetables growing on stonewool and their effects on activities of rhizosphere bacteria. Mol. Plant Microbe Interact. *19*, 250–256.

Kunkel, B.N., and Harper, C.P. (2018). The roles of auxin during interactions between bacterial plant pathogens and their hosts. J. Exp. Bot. *69*, 245–254.

Levy, A., Salas Gonzalez, I., Mittelviefhaus, M., Clingenpeel, S., Herrera Paredes, S., Miao, J., Wang, K., Devescovi, G., Stillman, K., Monteiro, F., et al. (2017). Genomic features of bacterial adaptation to plants. Nat. Genet. *50*, 138–150.

Li, J., Zhao-Hui, C., Batoux, M., Nekrasov, V., Roux, M., Chinchilla, D., Zipfel, C., and Jones, J.D. (2009). Specific ER quality control components required for biogenesis of the plant innate immune receptor EFR. Proc. Natl. Acad. Sci. USA *106*, 15973–15978.

Liao, C.Y., Smet, W., Brunoud, G., Yoshida, S., Vernoux, T., and Weijers, D. (2015). Reporters for sensitive and quantitative measurement of auxin response. Nat. Methods *12*, 207–210.

Lundberg, D.S., Lebeis, S.L., Paredes, S.H., Yourstone, S., Gehring, J., Malfatti, S., Tremblay, J., Engelbrektson, A., Kunin, V., Del Rio, T.G., et al. (2012). Defining the core Arabidopsis thaliana root microbiome. Nature *488*, 86–90.

Mashiguchi, K., Hisano, H., Takeda-Kamiya, N., Takebayashi, Y., Ariizumi, T., Gao, Y., Ezura, H., Sato, K., Zhao, Y., Hayashi, K.I., and Kasahara, H. (2019). Agrobacterium tumefaciens enhances biosynthesis of two distinct auxins in the formation of crown galls. Plant Cell Physiol *60*, 29–37.

McClerklin, S.A., Lee, S.G., Harper, C.P., Nwumeh, R., Jez, J.M., and Kunkel, B.N. (2018). Indole-3-acetaldehyde dehydrogenase-dependent auxin synthesis contributes to virulence of Pseudomonas syringae strain DC3000. PLoS Pathog *14*, e1006811.

Miyata, K., Kozaki, T., Kouzai, Y., Ozawa, K., Ishii, K., Asamizu, E., Okabe, Y., Umehara, Y., Miyamoto, A., Kobae, Y., et al. (2014). The bifunctional plant receptor, OsCERK1, regulates both chitin-triggered immunity and arbuscular mycorrhizal symbiosis in rice. Plant Cell Physiol *55*, 1864–1872.

Mucha, S., Heinzlmeir, S., Kriechbaumer, V., Strickland, B., Kirchhelle, C., Choudhary, M., Kowalski, N., Eichmann, R., Hückelhoven, R., Grill, E., et al. (2019). The formation of a camalexin biosynthetic metabolon. Plant Cell *31*, 2697–2710.

Patten, C.L., and Glick, B.R. (1996). Bacterial biosynthesis of indole-3-acetic acid. Can. J. Microbiol. *42*, 207–220.

Pieterse, C.M., Zamioudis, C., Berendsen, R.L., Weller, D.M., Van Wees, S.C., and Bakker, P.A. (2014). Induced systemic resistance by beneficial microbes. Annu. Rev. Phytopathol. *52*, 347–375.

Poole, L.B. (2005). Bacterial defenses against oxidants: mechanistic features of cysteine-based peroxidases and their flavoprotein reductases. Arch. Biochem. Biophys. *433*, 240–254.

Robert-Seilaniantz, A., Grant, M., and Jones, J.D. (2011). Hormone crosstalk in plant disease and defense: more than just jasmonate-salicylate antagonism. Annu. Rev. Phytopathol. *49*, 317–343.

Robinson, M.D., McCarthy, D.J., and Smyth, G.K. (2010). edgeR: a Bioconductor package for differential expression analysis of digital gene expression data. Bioinformatics *26*, 139–140.

Rosenberg, A., Sinai, L., Smith, Y., and Ben-Yehuda, S. (2012). Dynamic expression of the translational machinery during Bacillus subtilis life cycle at a single cell level. PLoS One *7*, e41921.

Sachs, J.L., Skophammer, R.G., and Regus, J.U. (2011). Evolutionary transitions in bacterial symbiosis. Proc. Natl. Acad. Sci. USA *108* (suppl 2), 10800–10807.

Schikora, S.T.S.A. (2015). Staining of callose depositions in root and leaf tissues. Bio-protocol *5*, e1429.

Schwessinger, B., Roux, M., Kadota, Y., Ntoukakis, V., Sklenar, J., Jones, A., and Zipfel, C. (2011). Phosphorylation-dependent differential regulation of plant growth, cell death, and innate immunity by the regulatory receptor-like kinase BAK1. PLoS Genet *7*, e1002046.

Song, Y., Wilson, A.J., Zhang, X.C., Thoms, D., Sohrabi, R., Song, S., Geissmann, Q., Liu, Y., Walgren, L., He, S.Y., and Haney, C.H. (2021). FERONIA restricts Pseudomonas in the rhizosphere microbiome via regulation of reactive oxygen species. Nat. Plants *7*, 644–654.

Spaepen, S., Bossuyt, S., Engelen, K., Marchal, K., and Vanderleyden, J. (2014). Phenotypical and molecular responses of Arabidopsis thaliana roots as a result of inoculation with the auxin-producing bacterium Azospirillum brasilense. New Phytol *201*, 850–861.

Spaepen, S., Vanderleyden, J., and Remans, R. (2007). Indole-3-acetic acid in microbial and microorganism-plant signaling. FEMS Microbiol. Rev. *31*, 425–448.

Spoel, S.H., and Dong, X. (2012). How do plants achieve immunity? Defence without specialized immune cells. Nat. Rev. Immunol. *12*, 89–100.

Stringlis, I.A., Proietti, S., Hickman, R., Van Verk, M.C., Zamioudis, C., and Pieterse, C.M.J. (2018). Root transcriptional dynamics induced by beneficial rhizobacteria and microbial immune elicitors reveal signatures of adaptation to mutualists. Plant J *93*, 166–180.

Teale, W.D., Paponov, I.A., and Palme, K. (2006). Auxin in action: signalling, transport and the control of plant growth and development. Nat. Rev. Mol. Cell Biol. *7*, 847–859.

Teixeira, P.J.P., Colaianni, N.R., Fitzpatrick, C.R., and Dangl, J.L. (2019). Beyond pathogens: microbiota interactions with the plant immune system. Curr. Opin. Microbiol. *49*, 7–17.

Teixeira, P.J.P.L., Colaianni, N.R., Law, T.F., Conway, J.M., Gilbert, S., Li, H., Salas-González, I., Panda, D., Del Risco, N.M., Finkel, O.M., et al. (2021). Specific modulation of the root immune system by a community of commensal bacteria. Proc. Natl. Acad. Sci. USA *118*, e2100678118.

Torres, M.A., Jones, J.D., and Dangl, J.L. (2005). Pathogen-induced, NADPH oxidase-derived reactive oxygen intermediates suppress spread of cell death in Arabidopsis thaliana. Nat. Genet. *37*, 1130–1134.

Tóth, K., and Stacey, G. (2015). Does plant immunity play a critical role during initiation of the legume-rhizobium symbiosis? Front. Plant Sci. *6*, 401.

Tsukagoshi, H., Busch, W., and Benfey, P.N. (2010). Transcriptional regulation of ROS controls transition from proliferation to differentiation in the root. Cell *143*, 606–616.

Van Puyvelde, S., Cloots, L., Engelen, K., Das, F., Marchal, K., Vanderleyden, J., and Spaepen, S. (2011). Transcriptome analysis of the rhizosphere bacterium Azospirillum brasilense reveals an extensive auxin response. Microb. Ecol. *61*, 723–728.

Wachsman, G., Zhang, J., Moreno-Risueno, M.A., Anderson, C.T., and Benfey, P.N. (2020). Cell wall remodeling and vesicle trafficking mediate the root clock in Arabidopsis. Science *370*, 819–823.

Wang, W., Chen, D., Zhang, X., Liu, D., Cheng, Y., and Shen, F. (2018). Role of plant respiratory burst oxidase homologs in stress responses. Free Radic. Res. *52*, 826–839.

Willmann, R., Lajunen, H.M., Erbs, G., Newman, M.A., Kolb, D., Tsuda, K., Katagiri, F., Fliegmann, J., Bono, J.J., Cullimore, J.V., et al. (2011). Arabidopsis lysin-motif proteins LYM1 LYM3 CERK1 mediate bacterial peptidoglycan sensing and immunity to bacterial infection. Proc. Natl. Acad. Sci. USA *108*, 19824–19829.

Wu, Y., Xun, Q., Guo, Y., Zhang, J., Cheng, K., Shi, T., He, K., Hou, S., Gou, X., and Li, J. (2016). Genome-wide expression pattern analyses of the Arabidopsis leucine-rich repeat receptor-like kinases. Mol. Plant *9*, 289–300.

Xie, S., Jiang, H., Xu, Z., Xu, Q., and Cheng, B. (2017). Small RNA profiling reveals important roles for miRNAs in Arabidopsis response to *Bacillus velezensis* FZB42. Gene *629*, 9–15.

Xin, X.F., Kvitko, B., and He, S.Y. (2018). Pseudomonas syringae: what it takes to be a pathogen. Nat. Rev. Microbiol. *16*, 316–328.

Zamioudis, C., Mastranesti, P., Dhonukshe, P., Blilou, I., and Pieterse, C.M. (2013). Unraveling root developmental programs initiated by beneficial Pseudomonas spp. bacteria. Plant Physiol *162*, 304–318.

Zhang, P., Jin, T., Kumar Sahu, S., Xu, J., Shi, Q., Liu, H., and Wang, Y. (2019). The distribution of tryptophan-dependent indole-3-acetic acid synthesis pathways in bacteria unraveled by large-scale genomic analysis. Molecules *24*, 19824–19829.

Zhao, Y. (2010). Auxin biosynthesis and its role in plant development. Annu. Rev. Plant Biol. *61*, 49–64.

Zhou, F., Emonet, A., Dénervaud Tendon, V., Marhavy, P., Wu, D., Lahaye, T., and Geldner, N. (2020). Co-incidence of damage and microbial patterns controls localized immune responses in roots. Cell *180*, 440–453.e18.

Zipfel, C. (2009). Early molecular events in PAMP-triggered immunity. Curr. Opin. Plant Biol. *12*, 414–420.

Zipfel, C. (2014). Plant pattern-recognition receptors. Trends Immunol *35*, 345–351.

Zipfel, C., Kunze, G., Chinchilla, D., Caniard, A., Jones, J.D., Boller, T., and Felix, G. (2006). Perception of the bacterial PAMP EF-Tu by the receptor EFR restricts Agrobacterium-mediated transformation. Cell *125*, 749–760.

Zipfel, C., Robatzek, S., Navarro, L., Oakeley, E.J., Jones, J.D., Felix, G., and Boller, T. (2004). Bacterial disease resistance in Arabidopsis through flagellin perception. Nature *428*, 764–767.

STAR★METHODS

KEY RESOURCES TABLE

REAGENT or RESOURCE	SOURCE	IDENTIFIER
Bacterial and virus strains		
Bacillus velezensis fzb42	BGSC	10A6
Paenibacillus polymyxa ATCC842	BGSC	N/A
Arthrobacter mf161	(Levy et al., 2017)	N/A
Bacillus velezensis fzb42 ΔysnE	BGSC	10A12
Bacillus velezensis fzb42 ΔysnE; amyE::P$_{ysnE}$ysnE (kan)	This study	N/A
Bacillus velezensis fzb42 ΔtrpAB	BGSC	10A10
Bacillus velezensis fzb42 ΔtrpED	BGSC	10A11
Bacillus velezensis fzb42 Δspf	https://www.nordreet.de/	N/A
Bacillus velezensis fzb42 ΔepsH	This study	N/A
Bacillus velezensis fzb42 ΔtasA	This study	N/A
Bacillus velezensis fzb42 ΔbslA	This study	N/A
Bacillus velezensis fzb42 ΔdegU	This study	N/A
Bacillus velezensis fzb42 ΔsinI	This study	N/A
Bacillus velezensis fzb42 Δhag	This study	N/A
Bacillus velezensis fzb42 ΔpnzL	This study	N/A
Bacillus velezensis fzb42 ΔyfnI	This study	N/A
Bacillus velezensis fzb42 ΔyfnF	This study	N/A
Bacillus velezensis fzb42; amyE::pSpac-GFP	https://www.nordreet.de/	N/A
Bacillus velezensis fzb42 recA::P$_{IPTG}$*recA*	This study	N/A
Bacillus velezensis fzb42 dabA::P$_{IPTG}$*dhbA*	This study	N/A
Bacillus velezensis fzb42 hemA::P$_{IPTG}$*hemA*	This study	N/A
Bacillus velezensis fzb42 ahpF::P$_{IPTG}$*ahpF*	This study	N/A
Bacillus velezensis fzb42 katA::P$_{IPTG}$*katA*	This study	N/A
Bacillus velezensis fzb42 ysnE::ysnE-GFP	This study	N/A
Chemicals, peptides, and recombinant proteins		
Horseradish Peroxidase	Thermo Fisher	Cat#31490
Luminol	Sigma	Cat#A8511
Diphenyliodonium chloride (DPI)	Sigma	Cat#43088
Indole acetic acid (IAA)	Sigma	Cat#I2886
Horseradish Peroxidase	Thermo Fisher	Cat#31490
Deposited data		
Plant RNA after *Bacillus velezensis fzb42* inoculation	This study	https://www.ncbi.nlm.nih.gov/bioproject/PRJNA718879
Bacillus velezensis fzb42 RNA O_2^- treatment	This study	https://www.ncbi.nlm.nih.gov/bioproject/PRJNA718895
Synthetic community 16s RNA	This study	https://www.ncbi.nlm.nih.gov/bioproject/742484
Experimental models: Organisms/strains		
Arabidopsis thaliana: WT Col-0	Benfey lab stock	NCBI:txid3702
Arabidopsis thaliana: *ein2-5*	ABRC	CS3071
Arabidopsis thaliana: *npr1-5*	ABRC	CS3724
Arabidopsis thaliana: *fls2*	ABRC	SAIL
Arabidopsis thaliana: *efr*	ABRC	SALK_068675

(*Continued on next page*)

Continued		
REAGENT or RESOURCE	SOURCE	IDENTIFIER
Arabidopsis thaliana: *lym1 lym3*	ABRC	CS2103242
Arabidopsis thaliana: *rbohd*	ABRC	CS68747
Arabidopsis thaliana: *rbohf*	ABRC	CS68748
Arabidopsis thaliana: *rbohd rbohf*	ABRC	CS68522
Arabidopsis thaliana: *tir1-1 afb4-8 afb2-3*	ABRC	CS69646
Arabidopsis thaliana: *jar1-1 axr1-3*	ABRC	CS67934
Arabidopsis thaliana: *myb51*	ABRC	CS421816
Arabidopsis thaliana: *axr5-1*	ABRC	CS16234
Arabidopsis thaliana: *cyp71a13*	ABRC	CS879462
Arabidopsis thaliana: *crt3*	ABRC	CS2103723
Arabidopsis thaliana: *pFRK1::NLS-3xmVENUS pUBQ10::RCI2A-tdTomato*	(Zhou et al., 2020)	Transgenic Col-0
Arabidopsis thaliana: *pPER5::NLS-3xmVENUS pUBQ10::RCI2A-tdTomato*	(Zhou et al., 2020)	Transgenic Col-0
Arabidopsis thaliana: *pEFR::NLS-3xmVENUS pUBQ10::RCI2A-tdTomato*	(Zhou et al., 2020)	Transgenic Col-0
Arabidopsis thaliana: *pFLS::NLS-3xmVENUS pUBQ10::RCI2A-tdTomato*	(Zhou et al., 2020)	Transgenic Col-0
Arabidopsis thaliana: *efr-2*	(Zipfel et al., 2006)	N/A
Arabidopsis thaliana: *bak1-5*	(Schwessinger et al., 2011)	N/A
Arabidopsis thaliana: DR5::GFP	(Liao et al., 2015)	N/A
Arabidopsis thaliana: DR5::GFP*; efr2*	This study	N/A
Software and algorithms		
DADA 2 version 1.16	(Callahan et al., 2016)	N/A
BlueBee Genomics Platform	(https://www.bluebee.com/lexogen)	N/A
Kallisto	(Bray et al., 2016)	N/A
EdgeR	(Robinson et al., 2010)	N/A

RESOURCE AVAILABILITY

Lead contact

Further information and requests for resources and reagents should be directed to and will be fulfilled by the Lead Contact Philip N. Benfey (philip.benfey@duke.edu)

Materials availability

Bacterial mutants and Arabidopsis lines generated in this study are available upon request.

Data and code availability

Arabidopsis Raw sequence reads were deposited in the SRA accession number: PRJNA718879. *B. velezensis* raw sequence reads were deposited in the SRA accession number: PRJNA718895. 16S raw sequence reads were deposited in the SRA accession number: PRJNA742484. Original/source data for the paper is available in Mendelely data https://doi.org/10.17632/8zyrz7ccbh.1]

EXPERIMENTAL MODEL AND SUBJECT DETAILS

Bacteria

B. velezensis Fzb42 bacteria and its mutant derivatives *ΔysnE*, *Δspf, ΔtrpAB, ΔtrpED* and *Paenibacillus polymyxa ATCC842* were purchased from the Bacillus genetic stock center (http://www.bgsc.org/). *Arthrobacter Mf161* was described previously (Levy et al., 2017). *B. velezensis amyE::pSpac-GFP* was purchased from NORDREET company (https://www.nordreet.de/). Other *B. velezensis* mutant strains including: ΔepsH, ΔtasA, ΔbslA, ΔdegU, Δhag, ΔpznL, ΔyfnI, ΔyfnF, ΔsinI, *ΔysnE amyE::*P_{ysne}*ysn*. IPTG inducible genes including: P_{IPTG}*recA*, P_{IPTG}*katA*, P_{IPTG}*ahpF*, P_{IPTG}*hemA*, P_{IPTG}*dhbA*, and y*snE-gfp* were generated in this study. The bacteria were cultivated routinely on Luria broth (LB) medium. When needed, the medium was solidified with 1.5% agar. For biofilm formation, bacteria were inoculated into MSgg medium and incubated without shaking for 4 days at 25° as described in (Branda et al., 2001). For experiments with IPTG inducible promoters (Figures 3B and S4B), 0.5mM IPTG was added to the growth media

30min before root inoculation, and later bacteria inoculated onto roots, on plates containing 0.5mM IPTG. For O_2^- treatment, bacteria were grown to OD_{600} = 1, then 0.5mM xanthine added and 5μl xanthine oxidase enzyme (Sigma) (Figures 3A, 3H, and S5A) or 0.5 enzyme for the RNA sequencing experiments.

Fungi

Rhizoctoinia solani isolate was kindly provided by Prof. Marc Cubeta (NCSU). Fungi were routinely grown on PDA plates (Sigma).

Plants

The Arabidopsis (Arabidopsis thaliana) SALK, SAIL and CS series of transfer DNA insertion lines of *ein2-5* (CS3071), *npr1-5* (CS3724), *fls2*_SAIL, *efr* (SALK_068675), *lym1 lym3* (CS2103242), *rbohd* (CS68747), *rbohf* (CS68748), *rbohd rbohf* (CS68522), *tir1-1 afb4-8 afb2-3* (CS69646), *jar1-1 axr1-3* (CS67934), *myb51* (CS421816), *axr5-1* (CS16234), *cyp71a13* (CS879462), and *crt3* (CS2103723) mutant alleles were purchased from the Arabidopsis Biological Resource Center (http://www.arabidopsis.org/). *efr-2* (Zipfel et al., 2006) and *bak1-5* (Schwessinger et al., 2011) are from Dangl lab stock. *pFRK1::NLS-3xmVENUS pUBQ10::RCI2A-tdTomato*, *pPER5::NLS-3xmVENUS pUBQ10::RCI2A-tdTomato*, and *pEFR::NLS-3xmVENUS pUBQ10::RCI2A-tdTomato*, and *pFLS::NLS-3xmVENUS pUBQ10::RCI2A-tdTomato*, were kindly provided by Prof. Niko Geldner (University of Lausanne). DR5::GFP*; efr2* line was generated in this study. All plants were grown on 0.5 MS media containing 1.1 gr Murashige and Skoog basal salts (in 500 ml ddH2O), 1% sucrose, 1% agar and 5 ml (in 500 ml ddH2O) MES (50 gr/l, pH=5.8 with NaOH). Plants were stratified for 2 d in a 4°C dark room and grown vertically for 4-10 days under long-day light conditions.

METHOD DETAILS

Bacterial genetic manipulation

The media and growth conditions used for DNA transformation of *B. velezensis* were described in (Idris et al., 2007). Gene deletions were performed by PCR amplification of 1000bp upstream and downstream of a given gene, the gene flanking regions were fused to an antibiotic resistance cassete using NEB builder (NEB) according to manufacturer's instructions. The reactions were amplified by PCR for 30 cycles and transformed into *B. velezensis*. *amyE::P_{ysne}ysnE* performed by PCR amplification of *ysnE* + 300bp upstream of *ysnE*, the PCR product fused to the upper and lower half of the *amyE* gene amplified by PCR using NEB builder (NEB) according to manufacturer's instructions. The reactions were amplified by PCR for 30 cycles and transformed into *B. velezensis*. Bacteria with IPTG inducible genes were generated by PCR amplification of 1000bp on either side of a gene and cloned with an antibiotic resistance cassette, pHyperSpac promotor [from pdr111 plasmid Pdr111 and antibiotic resistance cassete kindly provided by Prof. David Rudner (Harvard)] and the gene. The 4 fragments were fused together using NEB builder (NEB). The reaction was amplified by PCR for 30 cycles and transformed into *B. velezensis*. ysnE-gfp bacteria were generated by PCR amplification of *ysnE* without a stop codon, the GFP coding region from AR16 (Rosenberg et al., 2012), an antibiotic resistance cassette, and 1000bp downstream of *ysnE*. The 4 fragments were fused together and transformed into *B. velezensis*.

Monitoring bacterial growth on plant roots

Bacteria from fresh colonies were grown in LB medium to an OD_{600} = 1.0 and then diluted 1:100 in PBSx1 for CFU measurements and microscopy, or 1:10^3 for lateral roots and primary root measurements, yielding approximately 1×10^6, or 1x10^5 cfu/ml respectively. Six-day old seedlings were transferred onto square Petri dishes containing 0.5 MS but without sucrose. 2μL of bacterial dilution were put right above the root tip and left to dry for 2 min. The square plates were kept in a vertical position during the incubation time at 22°C under long-day light conditions (16 h light/8 h darkness) in a plant growth chamber. For bacterial CFU counting and microscopy, plants were incubated with bacteria for 48hrs. Then the inoculated plant roots were cut and washed three times in sterile water. For CFU counting the seedlings were transferred to a tube with 1 ml of PBSx1 and vortexed vigorously for 20 seconds, then the serial dilution was plated on LB plates. To asses the effect on EFR on *B. velezensis* colonization in the presence of the normal microbiota (Figure 6H), seedlings were inoculated with *B. velezensis amyE::pSpac-GFP (erm)* for 48 hrs and then transferred for non-sterile potting soil (Sun Gro horticulture) for 7d. 8 plants for each genotype, normalized for approximate rosette size were picked. The roots were excised, and normalized to 20 gr +/- 5%. The roots were washed 3 times, transferred to a tube with 10 ml of PBSx1 and vortexed vigorously for 20 seconds. then the serial dilution was plated on erm (1μg/ml) plates, and the number of GFP expressing bacteria was counted. Measuring callose deposition was done as described in (Schikora, 2015). For fungal infection, 6 day old seedlings grown on 0.5MS plates were inoculated with 10^{-3} CFU/ml of *B. velezensis* or buffer for 48 hrs, then a 5mm mycelial plug from the fungal culture was placed on the bottom of the plate and allowed to spread for an additional 7 days, after which, plant weight was measured. For estimation of fungal load, plant were treated as described above, after 3 days of fungal infection, seedlings were thoroughly washed for 20 times, and then transferred to a new agar plate. 24 hrs later the number of mycelia attached to the plant was quantifiy under the microscope. Seedling infected with fungus alone, without *B. velezensis* colonization were completely covered, precluding detailed quantification of fungal load (see Figure S9B). For syncom analysis the 34 bacteria were grown for over night at 30°, Streptomyces species were grown for 48 hrs. Then bacteria were adjusted to OD_{600} = 1, mixed together, centrifuged and resuspended in PBSx1. The mixed was diluted 1:100 in PBSx1 and inoculated as describes above. After 7 days the roots were excised, and treated and described above, then the PBSx1 was centrifuged and the supernatant freezed in -80°. Syncom DNA was extracted using PowerSoil DNA extraction kit (Qiagen). Library prepration and sequencing were done as described previously (Gohl et al., 2016). For sequence analysis Sequences were filtered and agglomerated into amplicon sequence variants (ASV) by DADA 2 version 1.16 (Callahan et al., 2016). *Arthrobacter MF161*'s ASV was identified based on 100% identity.

Microscopy

Roots were observed using a Zeiss LSM 880 laser scanning confocal microscope with the indicated lenses. Lateral root number was counted under a Zeiss Axio Zoom,V16 fluorescence dissecting scope at 10× magnification. Fluorescent intensity and length measurement were done using ImageJ.

Measurement of plant ROS production

Leaf discs were cut with a 4 mm biopsy punch from 4 week-old plants and placed on sterile water with their adaxial side up in a white 96-well microtiter plate (Costar, Fisher Scientific) containing 150 μl H_2O and then incubated overnight at 22°C in continuous light for 20 to 24 hours to reduce the wounding response. Immediately prior to elicitation, H_2O was removed from each well and 100 μl of the elicitation solution (100μg/ml HRP (sigma), 1μM luminol (sigma) and bacteria adjusted to OD_{600}=1) were added. Elicitation solution without bacteria was used as a control. Plates were analyzed every 1 min for a period of 45 min using a TECAN Infinite 200 PRO microplate reader with signal integration time of 0.5s. Statistical comparison between different plant genotypes was performed by Student t-test on maximal luminescence intensity values.

RNA extraction library preparation and computational analysis

For plant RNA, plant roots were cut and immediately frozen in liquid nitrogen. RNA prepared using RNeasy Plus Mini Kit (Qiagen) according to the manufacturer's instructions. RNA-seq libraries were prepared using QuantSeq 3' mRNA-Seq Library Prep Kit (Lexogen) according to the manufacturer's instructions. Illumina NextSeq 500 High-Output 75bp single reads were aligned to the *Arabidopsis thaliana* genome, and differentially expressed genes analyzed on the BlueBee platform (https://www.bluebee.com/lexogen) with default parameters. GO annotation was analyzed on (http://geneontology.org/) with default parameters.

For bacterial RNA preparation, bacteria treated with O_2^- for 30 min were precipitated and bacterial pellets immediately frozen in liquid nitrogen. Pellets were then resuspended in 500μl lysis buffer (30 mM Tris, 10 mM EDTA, 10 mg/mL lysozyme) for 30 min in 37°. RNA was prepared using the RNAzol reagent according to the manufacturer's instructions. rRNA was removed using NEBNext® rRNA Depletion Kit (Bacteria) according to the manufacturer's instructions. RNA-seq libraries were prepared using KAPA RNA HyperPrep Kit (Roche) according to the manufacturer's instructions.

Illumina MiSeq v2 150bp PE reads were aligned to *B. velezensis Fzb42* using Kallisto (Bray et al., 2016). Differentially expressed genes with logFC=0.5 and p-value < 0.01 were identified using the edgeR package. The full code was described in (Wachsman et al., 2020). Genes were annotated based on homology to the genome of *B. subtillis* 168, and GO annotation analyzed on (http://geneontology.org/) with default parameters with *B. subtillis* 168 based annotation. At least 72% of the differentially expressed genes from each comparision had homologs in the *B. subtillis* 168 genome.

QUANTIFICATION AND STATISTICAL ANALYSIS

All data analysis, and graphs were executed in Excel, except for RNA sequence analysis (see RNA extraction library preparation and computational analysis section below.) Two tailed t-test was applied for statistical comparison, with Bonferoni correction for multiple comparisons when relevant, or one way ANOVA followed by posthoc Tukey Kramer, as indicated in the relevant figure legends.